A NEW THREE-STAGE SCHEME FOR FINGERPRINT ENHANCEMENT AND ITS IMPACT ON FINGERPRINT RECOGNITION

Waziha Kabir

A Thesis

in

The Department

of

Electrical and Computer Engineering

Presented in Partial Fulfillment of the Requirements

for the Degree of Master of Applied Science (Electrical and Computer Engineering) at

Concordia University

Montreal, Quebec, Canada

August, 2013

CONCORDIA UNIVERSITY
SCHOOL OF GRADUATE STUDIES

This is to certify that the thesis prepared

By: Waziha Kabir

Entitled: "A New Three-Stage Scheme for Fingerprint Enhancement and Its Impact
            on Fingerprint Recognition"

and submitted in partial fulfillment of the requirements for the degree of

Master of Applied Science (Electrical and Computer Engineering)

Complies with the regulations of this University and meets the accepted standards with
respect to originality and quality.

Signed by the final examining committee:

_____ Chair
        Dr. M. Z. Kabir

_____ Examiner, External
        Dr. T. Fancott (CSE)   To the Program

_____ Examiner
        Dr. C. Wang

_____ Supervisor
        Dr. M. O. Ahmad

_____ Supervisor
        Dr. M. N. S. Swamy

Approved by: _____
                    Dr. W. E. Lynch, Chair
            Department of Electrical and Computer Engineering

_____20_____   _____
                                          Dr. C. W. Trueman
                                    Interim Dean, Faculty of Engineering
                                    and Computer Science

ABSTRACT

A NEW THREE-STAGE SCHEME FOR FINGERPRINT ENHANCEMENT AND ITS
IMPACT ON FINGERPRINT RECOGNITION

Waziha Kabir

In order to provide safety and security from fraudulent acts, it is necessary to use a reliable biometric identifier. Fingerprint is considered to be one of most effective biometric identifiers because of its universal characteristics. The recognition rate of identification/verification systems depends to a great extent on the quality of the fingerprint image. In a fingerprint recognition system, there are two main phases: 1) extraction of suitable features of fingerprints, and 2) fingerprint matching using those extracted features to find the correspondence and similarity between the fingerprint images. The low quality of fingerprint images provides false minutiae at the stage of feature extraction and reduces the recognition rate of minutiae-based fingerprint matching systems. Use of enhanced fingerprint images improves the recognition rate but at the expense of a substantially increased complexity. The objective of this research is to develop an efficient and cost-effective scheme for enhancing fingerprint images that can improve minutiae extraction rate as well as effectively improve the recognition rate of a minutiae-based fingerprint matching system.

In the first part of this thesis, a novel low-complexity three-stage scheme for the enhancement of fingerprint images is developed. In the first stage of the scheme, a linear

diffusion filter driven by an orientation field is designed to enhance the low-quality fingerprint image. The computational complexity is reduced by using a simple gradient-based method for estimating the orientation field and by using a small number of iterations. Although some of the broken ridges in the fingerprint image are partially connected after the first stage, this stage has a limitation of not being able to connect ridges broken with wide creases, and also not being able to recover ridges in the smeared regions. To overcome the shortcomings of the first stage, the fingerprint image obtained after the first-stage enhancement is passed through a compensation filter in the second stage. Although the broken ridges in the enhanced fingerprint image after the second stage are fully connected, the ridges affected by smears are only partially recovered. Hence, the output obtained from the second stage is passed through the third-stage enhancement, which has two phases: short-time Fourier transform (STFT) analysis and enhancement by an angular filter. In the first phase, a Gaussian spectral window is used in order to perform the STFT and this window helps to reduce the blocking effect in the enhanced image. In the second phase, the image obtained from the STFT is passed through an angular filter, which significantly improves the overall quality of the fingerprint image.

In the second part of this thesis, the effectiveness and usefulness of the proposed enhancement scheme are examined in fingerprint feature extraction and matching for fingerprint recognition applications. For this purpose, a minutiae extraction algorithm is first applied to extract minutiae from fingerprint images and then a minutia-based matching algorithm is applied to the set of extracted minutiae using a hybrid shape and orientation descriptor in order to find similarity between a pair of fingerprints.

Extensive experiments are conducted throughout this thesis using a number of challenging benchmark databases chosen from FVC2000, FVC2002 and FVC2004. Simulation results demonstrate not only the effectiveness of the proposed enhancement scheme in improving the subjective and objective qualities of fingerprint images, but also a superior minutiae extraction rate and a recognition accuracy of the fingerprint images enhanced by the proposed scheme at a reduced computational complexity.

ACKNOWLEDGEMENTS

It is my pleasure to express my sincere gratitude and thanks to my supervisors, Professor M.N.S. Swamy and Professor M. Omair Ahmad for their immense support, patience and brilliant guidance throughout my tenure in this thesis work. Their valuable suggestions and positive responses have been very useful, and were among the major reasons that enabled me to pursue my research. Their knowledge and expertise in the field enriches me a lot and opens new doors of thoughts and understanding to me. I feel extremely privileged to be able to work under their supervision.

Special thanks to my dear parents, who are the first inspiration for me in the field of research work. I am grateful for what they taught me about hard work and perseverance which are particularly essential in conducting research. I am grateful for their continuous support and prayers for me, which eased a lot of the hardships that faced. Dear parents, there are no enough words to describe my appreciation for both of you.

I would like also to thank all my other family members, my friends and my colleagues who supported me and were always available in times of need.

I would like to thank two researchers, Dr. JuCheng Yang and Dr. Carsten Gottschlich for their support in writing simulation codes of this research.

Finally, all praises and thanks to my Creator Who gave me the strength to successfully finish this thesis work.

TABLE OF CONTENTS

List of Figures

List of Tables

List of Symbols

A Test image

a Strength of Diffusion

B Template image

C Coherence image

C^{**} Cost of matching two minutiae for affine components

C^{γ} Cost of matching two minutiae for non-affine components

cn Crossing number

D Diffusion tensor

D_{be} Shape similarity distance for non-affine components

D_{SC}^{**} Total shape similarity distance

f Fingerprint image

G_x Horizontal Gradients

G_y Vertical Gradients

h Height of compensation filter window

h_{p_i} K-bin histograms of points p_i

h_{q_j}	K-bin histograms of points q_j
I_{FT}	First-stage enhanced image
I_{ST}	Second-stage enhanced image
I_{TS}	Third-stage enhanced image
K_c	Number of points on concentric circles
K_ρ	Gaussian kernel with variance ρ
K_σ	Gaussian kernel with variance σ
L	Number of concentric circles
M	Block mean
m_{A_i}	Minutiae points of test image
m_{B_j}	Minutiae points of template image
M_0	Desired mean
M_P	Multiplying factor
N	Normalized image
n	Number of iterations
$\mathbf{n}$	Normal vector
O	Dominant ridge orientation of the block

O_I	Improved orientation field
q	Quality metric
r_{min}	The outer boundary of the closest bin
r_δ	Tolerance for distortion differences
r_θ	Tolerance for angular differences
S	Similarity score
s	Symmetry image
T	Step size
t	Threshold
u	Filtered/enhanced fingerprint image
V	Block variance
V_0	Desired variance
v_1, v_2	Two orthonormal eigenvector
W	Spectral window
w	Width of compensation filter window
x	One dimensional signal
α, β	Contrast parameters

Ω	Rectangular domain
τ	Spatial position
τ_ρ	Structure tensor
λ	Eigenvalue
σ^2	Tunable parameter
δ_{max}	Maximum feasible distance
δ_S	Parameter to restrict similarity score
θ_{max}	Maximum feasible orientation
ω	Spatial frequency

List of Abbreviations

1-D   One-dimensional

2-D   Two-dimensional

AFVS   Automatic fingerprint verification system

AFIS   Automatic fingerprint identification system

ATM   Automated teller machine

DCT   Discrete cosine transform

DMR   Dropped minutiae ratio

EER   Equal error rate

EMR   Exchanged minutiae ratio

FFT   Fast Fourier transform

FMR   False match rate/ False minutiae ratio

FNMR   False non-match rate

FVC   Fingerprint verification competition

NIST   National institute of standards and technology

OF   Orientation field

ROC   Receiver operating characteristic

ROI   Region of interest

SFinGe   Synthetic fingerprint generation

STFT   Short time Fourier transform

SVD   Singular value decomposition

TMR   True minutiae ratio

USB   Universal serial bus

Chapter 1

Introduction

1.1 General

Biometrics is defined as the physiological and/or behavioural attributes of an individual, used to provide safety and security from fraudulent acts [1]. A biometric trait is reliable because of its properties, such as universality, uniqueness and permanence. Biometrics cannot be forgotten or lost, and because of its distinctive characteristics, it is more trustworthy than passwords, badge or USB keys. Biometrics can be classified into two categories: physiological, e.g., fingerprints, iris patterns, face, hand geometry and retinal blood vessels, and behavioral, e.g., voice, signature and keystroke dynamics. There are several applications of biometrics, for example, ATM and smart card security, online banking, immigration checkpoints, national ID, voter and driver registration. Biometric applications are rapidly growing in the sector of online banking due to the increasing number of electronic transactions, banking and commerce. A biometric recognition provides verification or identification of authenticated identities stored in databases based on some kind of unique features or characteristics possessed by an individual. The improvements of biometric technology are focusing on providing better recognition rate, security and cost effectiveness.

In a biometric system, the biometric data are acquired using a sensor and converted into a digital representation. The collected data are then stored in a biometric

database. Biometric templates are generated from the database and compare with an input template based on a similarity score and match using a pre-specified threshold. If the similarity score is more than the threshold, the result is a match, whereas, if the score is less than the threshold, the result is a non-match. Most of the biometric systems have two modes of operation: enrollment mode and identification mode. In the enrollment mode, templates are generated using some features and added to a database. In an identification mode, a template is generated for an individual using the same features as in the enrollment mode, and then a search is made for a match in the database of pre-enrolled templates. The basic block diagram of a biometric system is shown in Figure 1.1.

```
┌──────────┐                                                    ┌──────────┐
│ Biometric│                                                    │  Stored  │
│  Sensor  │                                                    │Templates │
└────┬─────┘                                                    └────┬─────┘
     │                                                               │
     ▼                                                               ▼
┌──────────┐   ┌──────────┐   ┌──────────┐    Test         ┌──────────┐
│   Pre-   │──▶│ Feature  │──▶│ Template │───────────────▶ │ Matcher  │
│processing│   │Extractor │   │Generator │                 └────┬─────┘
└──────────┘   └──────────┘   └──────────┘                      │
                                                                ▼
                                                          ┌──────────┐
                                                          │ Decision │
                                                          └──────────┘
```
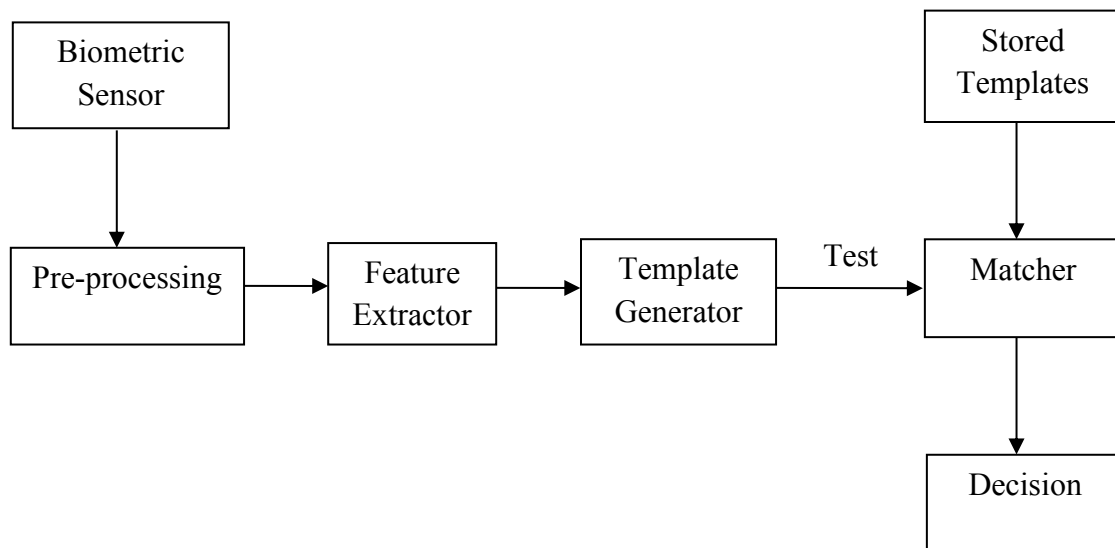
Figure 1.1 The basic block diagram of a biometric system [1]

Fingerprint is the oldest and most widely used biometric identifier. Reliable minutiae extraction is a critical step in an automatic fingerprint identification. However, reliability of minutiae extraction heavily depends on the quality of the input fingerprint

image. The robustness of minutiae extraction can be improved by incorporating an enhancement algorithm in fingerprint recognition systems.

1.2 Literature Review of Fingerprint Enhancement Techniques

There are several existing algorithms to enhance the quality of fingerprint images [1-28]. In general, fingerprint enhancement algorithms can be classified into two categories: spatial-domain and frequency-domain enhancement.

1.2.1 Spatial-domain Enhancement

In a spatial-domain technique, an enhanced image is obtained by convolving the input fingerprint image with a spatial filter mask. The size of the mask dictates the computational complexity of the filtering process.

In the spatial-domain, the most popular algorithm for fingerprint enhancement proposed by Hong et al. [2] is based on the directional Gabor filtering kernel [1]. The authors model the gray levels along the ridges and valleys of a fingerprint as a sinusoidal-shaped wave having a direction orthogonal to the ridge orientation. The local ridge frequency is considered as sinusoidal-shaped wave and computed pixel-wise. The filtering kernel proposed in [2] is both frequency-selective and orientation-selective, which makes it to give maximal responses to ridges at a specific orientation and frequency in the fingerprint image. However, there are some limitations of this algorithm: 1) the ridge frequency is not a sinusoidal-shaped wave in real fingerprint image, 2) the estimated frequency may be incorrectly estimated for the presence of noise, broken ridges, scars, etc in the fingerprint image, and 3) the parameters need to be selected empirically depending on specific databases. In addition, this method requires accurate

contextual information (local ridge orientation and frequency) and suffers from artifacts near high curvature and singularity areas.

Yang et al. [3] have modified the traditional Gabor filter by discarding the assumption of the grey-levels along the ridges and valleys to have a sinusoidal plane wave model. The authors assumed that the ridge and valley structures follow a plane wave consisting of two cosinusoidal functional curves of two different frequencies. The parameters of this modified Gabor filter are selected adaptively. The proposed method fails to enhance the fingerprint image if it consists of unrecoverable regions.

Areekul et al. [4] proposed generalized separable Gabor filters to deal with any orientation of fingerprint image. In this technique, Gabor filter is divided into high-pass and low-pass segments to improve the filtering process. The method performs a separable convolution after interpolating consecutive sequences of pixels along an arbitrary direction. Although the computational complexity is less than that of the traditional Gabor filter method by Hong et al. [2], there are errors in the enhanced images because of the inaccurate Gabor features.

Yun and Cho [5] proposed an adaptive preprocessing method for fingerprint recognition based on clustering the quality of fingerprint images. The input fingerprint images are clustered into three categories: oily, neutral and dry based on five extracted features (i.e., mean, variance, block directional difference, ridge-valley thickness ratio and orientation change). Then, the ridges and the valleys of the dry and the oily clustered fingerprints, respectively, are enhanced with adaptive filters. The images clustered as neutral are considered to be good quality fingerprints, and thus, there is no need to

enhance them. Then, ridge and valley enhancement is applied to dry and oily images, respectively, to enhance these two types of fingerprint images. However, this method fails to enhance fingerprint images containing smears and broken ridges.

Hastings [6] developed a method to enhance a ridge using an iterative smoothing anisotropic diffusion process along the direction of the ridge orientation. The anisotropic diffusion filter adapts to smooth the image only in the direction parallel to the ridge flow. The image intensity varies smoothly and, most of the small irregularities and breaks are removed. However, this method produces blurring effects in the enhanced images and thus, destroys the ridge structures.

Zhao et al. [7] proposed an oriented non-linear diffusion driven by the ridge curvature and singular points. First, singular points are detected iteratively based on Poincare index [1]. Second, the orientation field is regularized using a singularity driven non-linear diffusion process. Finally, an oriented diffusion process driven by curvature and singular points is applied to enhance the oriented patterns. The performance of this method is good in the region of curvature and singular points, but the iterative process to locate the singular points increases the computational complexity.

Gottschlich and Schönlieb [8] proposed a modified diffusion-based method to enhance low-quality fingerprint images. Previously, a diffusion tensor was derived from the image gradients only. The diffusion tensor of the method proposed in [8] is derived from a pre-computed orientation field along with the image gradient. The orientation field is computed by a combination of two orientation field estimation methods: the line sensor method and the gradient based method. A comparison is performed between the

two estimation methods and a threshold is applied to obtain the final orientation. Then, the computed orientation field is fed to the diffusion tensor to perform the filtering process. Finally, a local contrast enhancement technique is applied to improve the contrast of the fingerprint images, what is reduced as a result of diffusion process. Forty iterations are used to obtain an enhanced fingerprint image. However, the computational complexity is high due to the processes of estimating the orientation field and performing the iterative diffusion.

1.2.2 Frequency-domain Enhancement

In a frequency-domain technique, an enhanced image is obtained by convolving the input fingerprint image with the frequency domain filter. The convolution in the spatial domain is equivalent to a multiplication operation in the frequency domain.

Sherlock et al. [9] have proposed a non-stationary directional filter for enhancing fingerprint images in the frequency domain. A fingerprint image is convolved with precomputed filters located at eight directions with the intervals of 22.5 degrees resulting in a set of filtered images. The enhanced image is reconstructed by a selecting each pixel direction of the filtered images that corresponds most closely to the actual ridge orientation obtained from the original fingerprint image. Finally, a thresholding technique is used to obtain binary enhanced image. The algorithm assumes that the ridge frequency is constant. Therefore, the proposed method does not utilize the full contextual information provided by the fingerprint image. In addition, the algorithm requires to compute a large number of precomputed filters to enhance the fingerprint image. Thus, the computational complexity is quite high and thus, not suitable for real-time applications.

Chikkerur et al. [10] have presented a directional bandpass filter for enhancing fingerprint images in the frequency domain based on short time Fourier transform (STFT) analysis. The bandpass filter proposed in [10] has two separate filters: radial filter and angular filter. The input fingerprint image is divided into blocks, and the ridge orientation and frequency are approximated probabilistically for each block. Then, the radial and angular filters are obtained at the center of the ridge frequency and orientation, respectively. The block fingerprint images are filtered by both the radial and angular filters to obtain block enhanced images. Finally, the enhanced image is reconstructed combining all the block enhanced images. Although the probabilistic approximation removes impulse noise (small gaps on ridges or dots in valleys), this algorithm fails to enhance the unrecoverable regions of fingerprint images.

Jirachaweng and Areekul [11] proposed an overlapped block-based discrete cosine transform (DCT) instead of a Fourier transform to reduce the computational complexity. The proposed bandpass filter in [11] in the DCT domain consists of ridge frequency and orientation filters. The ridge frequency filter is centered at the ridge frequency, which is obtained by measuring the distance between the origin and the highest DCT peak of the high frequency spectrum. The ridge orientation filter is centered at the ridge orientation, which is the peak angle in DCT coefficients and measured counterclockwise from the horizontal axis to the terminal side of the highest spectrum peak of high frequency. Then, the input image is filtered using the bandpass filter in the DCT domain to obtain the enhanced fingerprint image. This method requires accurate contextual information (local ridge orientation, frequency, angular bandwidth). The

drawbacks of this method are blocking artifacts around singular regions. Also, the effectiveness of the algorithm is not studied for low quality fingerprint images.

The method of Hsieh et al. [12] is based on wavelet decomposition to enhance fingerprint images using both global textural information and local ridge orientation. The fingerprint images are decomposed using wavelet into sub-images. The sub-images are filtered based on a voting technique by a series of textural and directional filters. The enhanced image is then obtained by reconstructing process using wavelet transform. This algorithm suppresses the spectral noise and connects the broken ridges produced by creases and scars. However, this method with a textural filtering requires high computational time due to wavelet transform.

Zhang et al. [13] combined the Gabor filter method in [2] with the wavelet transform. The wavelet coefficient set is adjusted using a map function in order to reduce the noise in a fingerprint image. Then, the Gabor filter is applied to further enhance the ridge using the orientation and frequency information of the fingerprint image. However, this method is less effective in improving the contrast between ridges and valleys in fingerprints containing singular points (e.g., delta).

Lei et al. [14] have proposed a non-tensor wavelet filter banks for decomposing fingerprint images in order to obtain wavelet coefficients. Then, they use an anisotropic filter to modify the approximation subimage and apply an adaptive approach to adjust the high frequency coefficients of the other three subimages. Finally, the inverse transform is applied, followed by a contrast enhancement stage to obtain the enhanced fingerprint image. Due to the combination of wavelet transform and anisotropic diffusion filters, the

execution time is more than that of the individual filtering approaches. Also, the diffusion tensor is computed from the gradients of the fingerprint image, and thus makes the anisotropic diffusion filtering less effective.

Yang et al. [15] have utilized both spatial and frequency domain filtering to enhance low quality fingerprint images. The spatial domain filter, which is an iterative one, is computed from local ridge orientation of the input fingerprint image, is followed by the frequency domain filter that consists of a raised cosine angular filter and exponential bandpass radial filter. Although this method enhances the quality of singular point and high curvature regions, the performance relies on context extraction and the execution time is high due to the iteration applied at the stage of the spatial domain filtering.

Sutthiwichaiporn et al. [16] have proposed an enhancement algorithm based on spatial partitioning and frequency domain filtering approach. The input fingerprint image is pre-processed depending on the type of sensor used to locate the region of interest (ROI). The ROI is partitioned based on the quality of blocks and these blocks are rearranged in order of priority for frequency domain filtering. The high-quality blocks are enhanced first and the lower quality blocks neighboring enhanced blocks are iteratively enhanced later. Finally, all the enhanced blocks are combined to reconstruct the enhanced fingerprint image. The limitation of this method is the requirement of segmentation, and it fails to enhance fingerprint images having strong crack and noise.

1.3 Motivation

The performance of a fingerprint recognition technique depends on the quality of the fingerprint image. A low-quality fingerprint image creates spurious minutiae at the stage of feature extraction. It leads to a performance degradation of fingerprint matching. A low-quality fingerprint image is characterized by dryness, wetness, scars and so on. A fingerprint is dry due to the low temperature or lack of natural moisture in the skin, which produces broken ridges in the fingerprint image. The wetness of a fingerprint caused by the presence of excessive moisture in the skin, and it leads to conglutinated ridges in the fingerprint image. Scars are the evidences of a trauma, which leaves marks on the fingertip and they create interruption in the natural flow of fingerprint ridges. Figure 1.2 shows some examples of poor-quality fingerprint images.

Dry   Wet   Scarred

Figure 1.2 Some examples of poor-quality fingerprint images

The motivation behind the fingerprint image enhancement is to improve the quality of the fingerprint images so that the true minutiae extraction rate increased. The minutiae extracted from the fingerprint image depend upon the quality of the input fingerprint. In order to extract true minutiae, we thus require enhancing the quality of fingerprint images.

Most of the enhancement algorithms discussed in Section 1.1 suffers from high computation complexity. Thus, computationally efficient enhancement algorithms are required to improve the quality of the fingerprint image.

1.4 Objectives of the Thesis

In order to provide a good fingerprint recognition, an enhancement method is required, to improve the quality of fingerprint images (e.g. fingerprint images in databases FVC2004 [30] and FVC2006[1]) and very low quality prints (e.g., latent fingerprint images in NIST SD27 [31]). There are several enhancement algorithms [1]-[28] that have been proposed for fingerprint images in recent years. Enhancing fingerprint images is quite different from a general image enhancement. Improving minutiae extraction and recognition rate are the main goals in enhancing fingerprint images. An aggressive or weak enhancement algorithm may create spurious minutiae leading to poor recognition rate. Thus, devising an appropriate enhancement algorithm is a challenging task.

The objective of this thesis is to develop a computationally efficient filtering scheme to improve low-quality fingerprint images. A novel three-stage fingerprint image enhancement scheme that uses both spatial and frequency domain filtering is proposed. The proposed scheme makes use of a corrected orientation field for its diffusion filter and

---

[1]This database is not publicly available.

11

a new and effective angular filter for its Gaussian filter. The emphasis in this work is to connect broken ridges, remove scars and smears, separate conglutinated ridges, and improve the contrast in fingerprint images. It aims at enhancing the quality of fingerprint images with a view to a better extraction of true minutiae and an improved fingerprint recognition rate.

The novelties of the proposed method are; 1) it uses a corrected orientation field for the diffusion filter in the first stage, 2) a non-iterative compensation filter in the second stage, and (3) a new and effective Gaussian angular filter in the third stage.

1.5 Organization of the Thesis

This thesis is organized as follows.

In Chapter 2, a background material necessary for the development of the work undertaken in this thesis is presented. The contextual information to drive a fingerprint recognition system, metrics used for the performance evaluation and details of the different databases used to obtain the experimental results are discussed. The basic of anisotropic diffusion filtering technique is also explained.

In Chapter 3, a novel three-stage fingerprint enhancement scheme is developed. In the first stage, by using a linear anisotropic diffusion filter, a preliminary enhanced fingerprint image is obtained, which is used to estimate an enhanced orientation field. This preliminary enhanced image along with the improved orientation field is then employed by a compensation filter in the second stage in order to further enhance the image. Finally, in the third stage, a new angular filter is devised to obtain the final enhanced fingerprint image. Extensive experiments are conducted to assess the

performance of the proposed method in enhancing fingerprint images from benchmark databases and the results compared with that of some of the state-of the-art techniques showing the effectiveness of the method proposed in this thesis.

In Chapter 4, the impact of the proposed scheme for fingerprint enhancement is examined in fingerprint minutiae extraction and in fingerprint matching problems. Minutiae are extracted from the enhanced images obtained from the proposed method. A matching algorithm is performed with those extracted minutiae in order to find the similarity between two fingerprints. The true minutiae extraction ratio and recognition rates are computed for the proposed method and the results compared with that of some of the state-of the-art schemes.

Finally, Chapter 5 concludes the thesis by summarizing the contributions of the work undertaken and by providing some suggestions for future investigation.

Chapter 2

Background Material

2.1 Introduction

In this chapter, the background material required to develop the work undertaken in this thesis is discussed. In Section 2.2, fingerprint recognition systems are described. In Section 2.3, types of features within fingerprint images are discussed, followed by the extraction of these features and their matching in Section 2.4. There are several metrics used to measure the system performance, and these are discussed in Section 2.5. The databases used for the various experiments performed in this thesis are described in Section 2.6. Finally, in Sections 2.7 and 2.8, the anisotropic diffusion process and short time Fourier transform (STFT) analysis used in fingerprint image processing are briefly described.

2.2 Fingerprint Recognition Systems

Fingerprints are basically patterns of two line structures, called ridges and valleys, on the surface of a fingertip. The persistent dark lines are known as ridges and the white pixels between ridges are known as valleys. Each individual has unique fingerprints, even for identical twins. A fingerprint of an individual does not change with time except for bruises, scars, etc. caused by an accident. Fingerprint recognition systems have become very popular and reliable due to these characteristics of fingerprints.

Fingerprint recognition systems may be classified into two categories: (1) automatic fingerprint verification system (AFVS) and (2) automatic fingerprint identification system (AFIS).

(1) An automatic fingerprint verification system (AFVS) determines the identity of an individual by comparing the captured fingerprint with previously stored fingerprint template(s) of that individual in a database. AFVS performs a one-to-one comparison to justify as to whether the identity claimed by that individual is true or not. A verification system accepts the claimed identity as a genuine match or rejects it as an imposter match.

(2) An automatic fingerprint identification system (AFIS) recognizes the identity of an individual by searching the entire fingerprint database. AFIS performs one-to-many comparisons for a match to establish the identity of that individual. If the claimed identity is present in the database, the identification system returns a genuine match as a result; otherwise it rejects the identity claimed by that individual as an imposter match.

There is a common stage for both verification and identification systems as explained below:

- Enrollment Stage: This stage is to enter a new identity of an individual in the system database. A sample of the individual fingerprint is captured by a sensor at first. The captured sample is then used for extracting features leading to the creation of templates. Finally, this template is stored in the system database that is used for either verification or identification.

The block diagram of a fingerprint recognition system is depicted in Figure 2.1. As seen from this figure, the only difference between verification and identification systems is the characteristic of matching. The verification and identification processes consist of the following four major modules:

- Acquisition: In this stage, raw fingerprints are acquired using a sensor, known as scanner.

- Pre-processing: Acquiring a good contrast fingerprint image directly from an acquisition device is not always possible because of the limitations of these devices and improper illumination conditions of the surroundings. Thus, pre-processing is applied to improve the quality of the raw fingerprint images.

- Feature Extraction: Extracting prominent features from fingerprint image for the creation of templates and to facilitate verification or identification processes.

- Matching: Comparing the extracted template against a reference template in terms of a matching score based on a threshold to make the final decision (a match or a non-match). The matching modules of AFVS and AFIS conduct one-to-one and one-to-many comparisons, respectively.

2.3 Fingerprint Features

The required information for fingerprint matching is carried by distinctive fingerprint features, which can be divided into two categories: global features (i.e., singular points and ridge orientations) and local features (i.e., minutiae) [32].

Global Features

- *Local ridge orientation* is the angle between a local ridge at a pixel and the horizontal axis. The set of these ridge orientations collectively is known as the orientation field (OF) or directional image of the fingerprint image. There are several methods proposed for computing the orientation field [1]. Amongst all these methods, the most popular technique is one proposed by Ratha et al. [33] based on gradients of the fingerprint image. The ridge orientation is computed for each nonoverlapping block of size $W \times W$. For each pixel, the orientation corresponds to the most dominant ridge direction of the block. The block orientation $O(i,j)$ is determined as:

$$O(i,j) = \frac{1}{2}\tan^{-1}\left(\frac{\sum_{u=i-\frac{W}{2}}^{i+\frac{W}{2}} \sum_{v=j-\frac{W}{2}}^{j+\frac{W}{2}} 2G_x(u,v)G_y(u,v)}{\sum_{u=i-\frac{W}{2}}^{i+\frac{W}{2}} \sum_{v=j-\frac{W}{2}}^{j+\frac{W}{2}} G_x^{\,2}(u,v)G_y^{\,2}(u,v)} \right) \qquad (2.1)$$

where $G_x(u,v)$ and $G_y(u,v)$ are the horizontal and vertical gradients, respectively, obtained using 3×3 Sobel mask as gradient operator.

- *Local ridge frequency* indicates the density of the ridges in a fingerprint image obtained by computing the average inter-ridge distance within a block. The frequency of the ridges varies across the different regions of a fingerprint image. Several methods have been proposed to compute the ridge frequency [1].
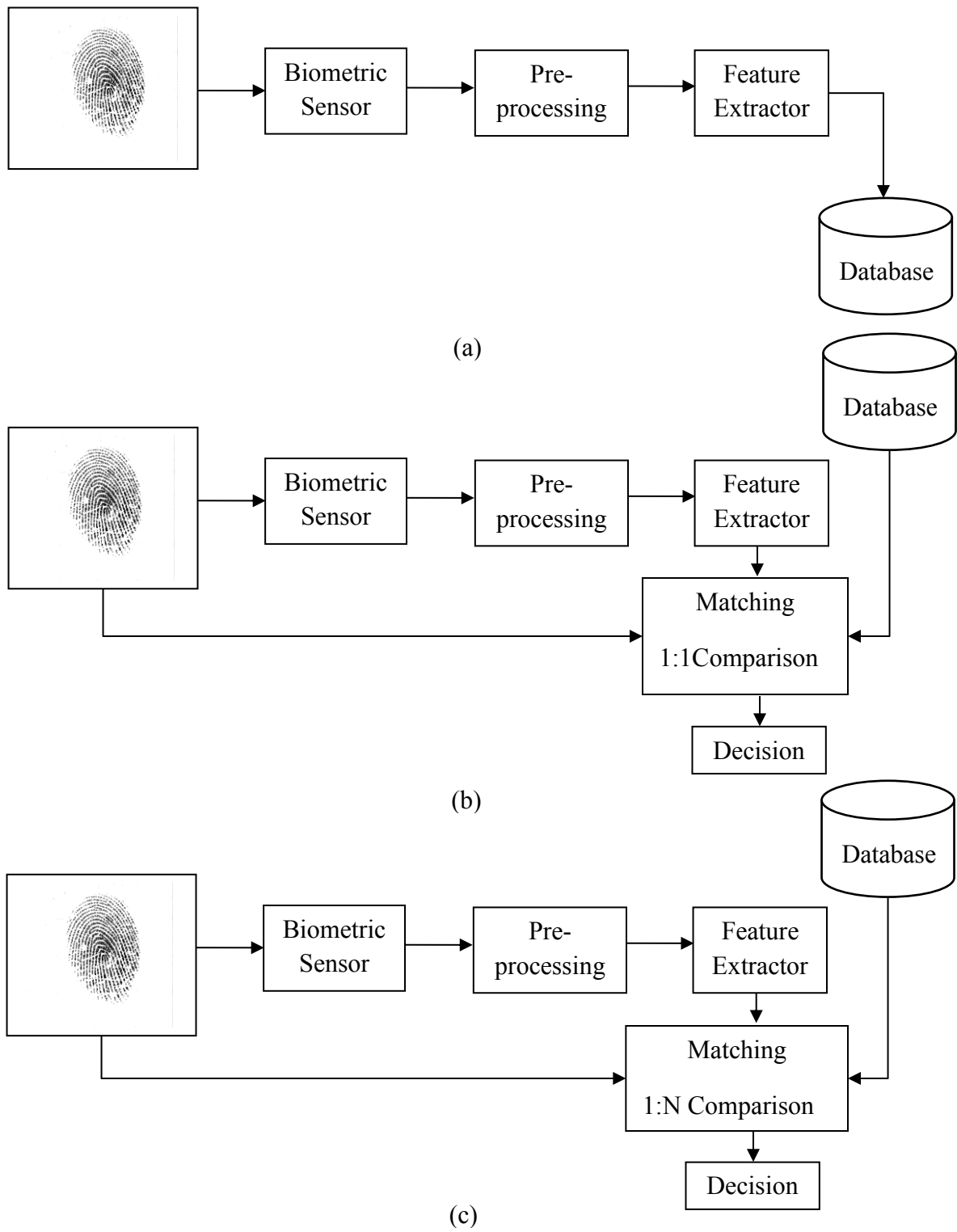
Figure 2.1 Basic block diagrams of fingerprint recognition systems, (a) Enrollment process,
(b) Verification process and (c) Identification process

- *Singular points* are mainly of two types: core and delta, where the ridge orientation vanishes or is discontinuous. Fingerprint images can be classified into six classes based on singular points, as shown in Figure 2.2.

| Arch | Tented arch | Left loop |

| Right loop | Whorl | Whorl (Twin loop) |
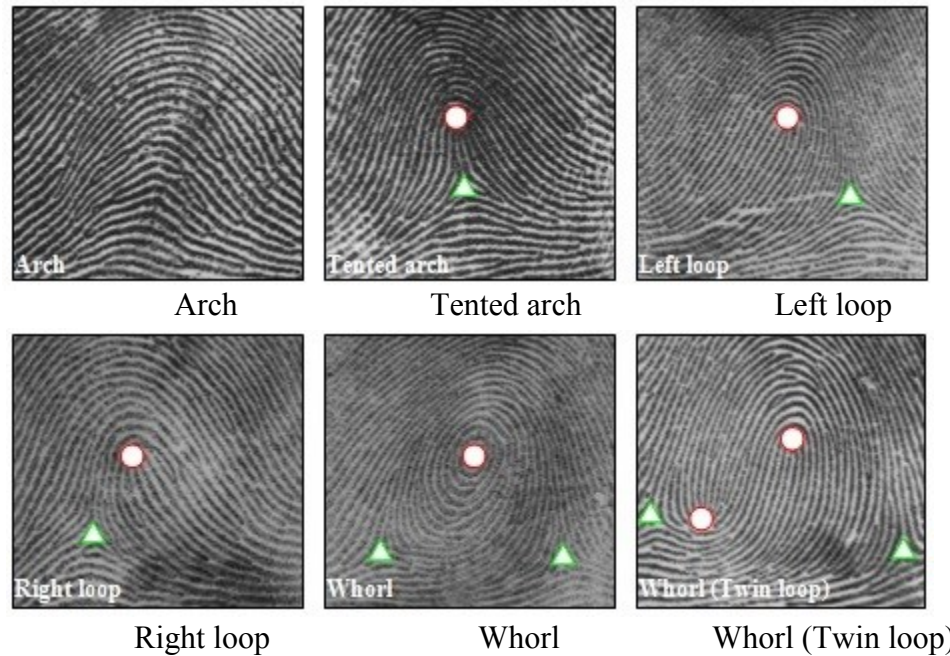
Figure 2.2 Various types of fingerprints with the cores (marked as circle) and the deltas (marked as triangle) [1].

Local Features

Minutiae are the local features of a fingerprint, which are unchanged over an individual's lifetime [28]. There are several types of minutiae, but the two most prominent minutiae are those characterized ridge ending and ridge bifurcation, as shown in Figure 2.3. A ridge ending minutia is defined as the point where the ridge terminates abruptly and a ridge bifurcation minutia is the point where the ridge is divided into branches. Typically, there are about 40-100 minutiae within a good-quality fingerprint image [2].

2.4 Fingerprint Feature Extraction and Matching

The fingerprint features discussed in Section 2.3 are extracted to generate the template of a fingerprint image. These features may be extracted based on ridge flow or structure, and the location, orientation and type of minutiae within the fingerprint image.

Fingerprint matching is a process of comparison between the templates of two fingerprints. The matching scheme returns a similarity score in the range of 0 to 1. The matching decision depends on a threshold. If the similarity score is more than a specified threshold, the result is a match; otherwise, the matching scheme returns a non-match that is, when the score is lower than the threshold.

2.5 Metrics used for Performance Evaluation

The performance of a fingerprint enhancement algorithm is measured based on three main factors:

1) *Quality Estimation* measures the quality of the enhanced fingerprint image. In general, there exists two types of quality estimation methods: global quality estimation and local quality estimation [1]. The quality estimation methods may be devised based on the consistency of local orientation, intensity of the pixels, frequency and thickness of the ridges, and so on.

2) *Computational Complexity* is the execution time to run an enhancement algorithm. Two other time measurements are: enrollment time and matching time. The enrollment time is defined as the time needed to perform pre-processing,

feature extraction and template formulation (Figure 2.1 (a)). The matching time is

the required time to compare two different templates.
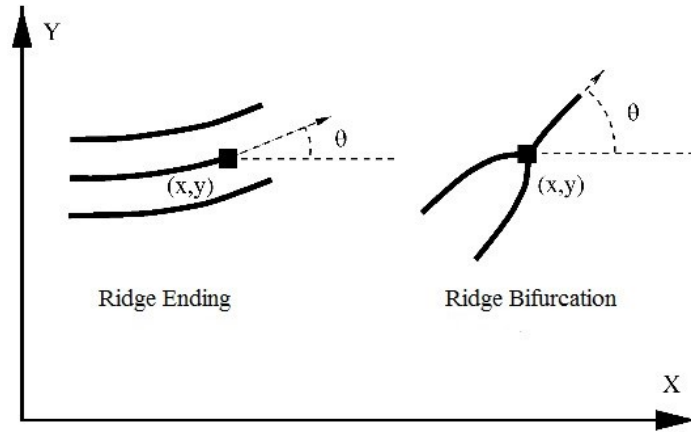
(a)
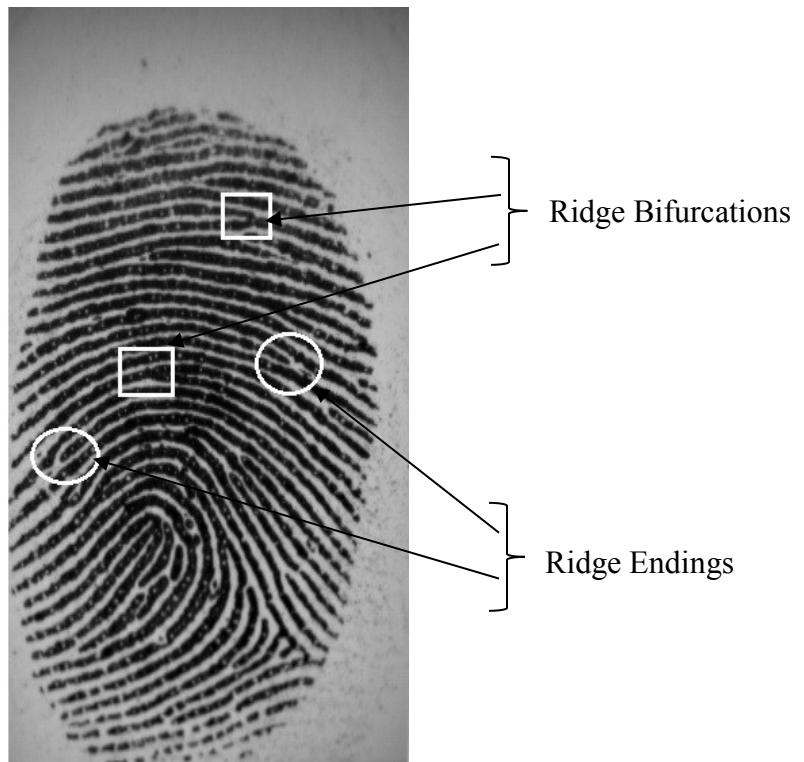
(b)

Figure 2.3 Examples of minutiae. (a) two types of minutiae with their location and
orientation [2], (b) minutiae marked (squares and circles) on a fingerprint image.

21

3) *Recognition Rate* defines the accuracy of the decision of a fingerprint system. In order to obtain the recognition rate, there are mainly three types of error rates to be computed: false match rate (FMR), false non-match rate (FNMR) and equal error rate (EER). FMR occurs when a matching algorithm classifies an actual imposter as a genuine one through the process of comparison of two templates. FNMR is the result of classifying genuine one as an imposter by the matching scheme. FMR and FNMR, computed using similarity score, given by:

$$FMR = \frac{N_{AI}}{N_I} \times 100$$

$$FNMR = \frac{N_{RG}}{N_G} \times 100$$

(2.2)

where N_{AI} is number of accepted imposters, N_I is the number of imposter attempts, N_{RG} is the number of rejected genuine, and N_G is the number of genuine attempts. The equal error rate (EER) is defined as the error rate at the threshold t when FMR = FNMR. The system performance is also reported at all operating points (threshold t), by plotting FMR(t) against FNMR(t) as a receiver operating characteristic (ROC) curve as shown in Figure 2.4.

2.6 Details of Databases

In this section, the databases used for the experiments performed within this thesis are described. The databases from fingerprint verification competition (FVC), namely, FVC2000 [35], FVC2002 [36], and FVC2004 [30], which are publicly available, are used for different experiments throughout this research. Each of these FVCs contains four different sub-databases, DB1, DB2, DB3 and DB4. The first three consist of real

fingerprint images acquired by different types of sensors and the fourth one contains synthetic fingerprint images created by a Synthetic Fingerprint Generator (SFinGe). Each of the sub-databases contains two sets, namely, A and B. There are 800 fingerprints (100 fingers with 8 impressions for each finger) for the set A and 80 fingerprints (10 fingers with 8 impressions for each finger) for the set B. The fingers numbered 1 to 100 (set A) have been selected for testing and estimating the parameter values, and the rest of the fingers, numbered 101 to 110 (set B), are used for training. Tables 2.1, 2.2 and 2.3 provide a summary in terms of the fingerprint size, resolution and the source of acquisition of the FVC databases [30, 35-36].
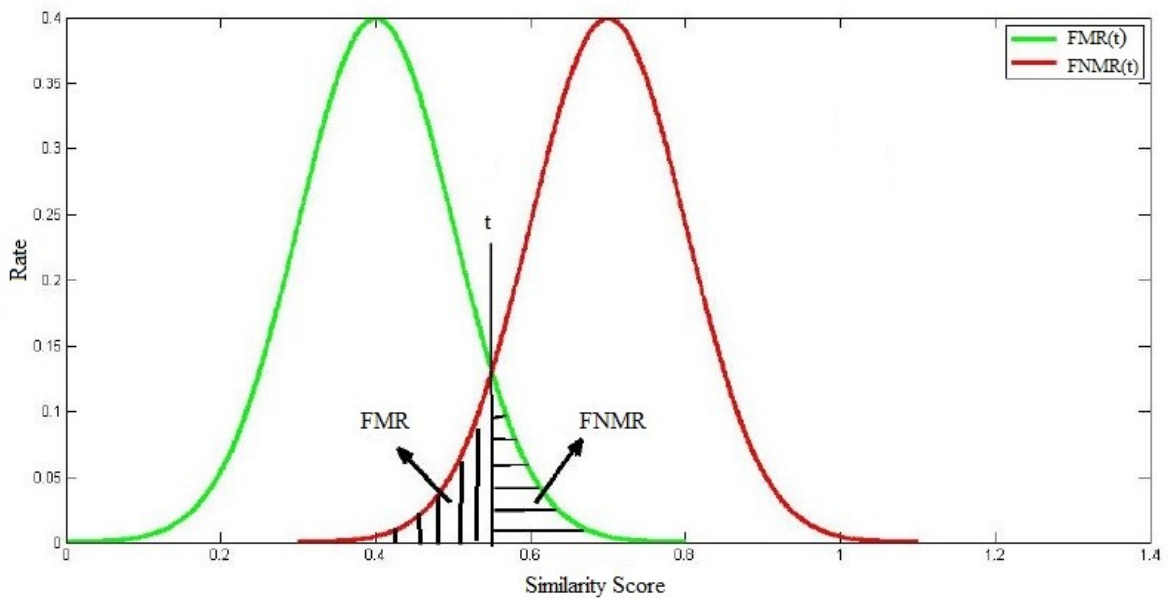
Figure 2.4 FMR and FNMR for a given threshold t [34].

Table 2.1 Summary of FVC2000 database [35]

Sub-database	Type of Sensor	Size of Image	Resolution of Image
DB1	Optical	300×300	500
DB2	Capacitive	256×364	500
DB3	Optical	448×478	500
DB4	SFinGe	240×320	~500

Table 2.2 Summary of FVC2002 database [36]

Sub-database	Type of Sensor	Size of Image	Resolution of Image
DB1	Optical	388×374	500
DB2	Optical	296×560	569
DB3	Capacitive	300×300	500
DB4	SFinGe v2.51	288×384	~500

Table 2.3 Summary of FVC2004 database [30]

Sub-database	Type of Sensor	Size of Image	Resolution of Image
DB1	Optical	640×480	500
DB2	Optical	328×364	500
DB3	Thermal sweeping	300×480	512
DB4	SFinGe v3.0	288×384	~500

2.7 Basic of Anisotropic Diffusion Filtering

The most recent anisotropic diffusion filter for fingerprint image processing is proposed by Gottschlich and Schönlieb [8]. Let the fingerprint image f be defined on a rectangular domain $\Omega \subset \Re^2$ and $u = u(x,t):\Omega \times (0,\infty) \rightarrow \Re$ be the set of filtered/enhanced fingerprint images obtained from the solution of the diffusion equation given by [8]

$$\begin{cases} \dfrac{\partial u}{\partial t} = div(D\nabla u) & on \quad \Omega \times (0,\infty) \\ u(x,t=0) = f(x) & on \quad \Omega \\ \langle D\nabla u, n \rangle & on \quad \partial\Omega \times (0,\infty) \end{cases} \qquad (2.3)$$

where $D \in \Re^{2\times2}$ is diffusion tensor and $\mathbf{n}$ denotes outer normal vector on $\partial\Omega$. The diffusion tensor is constructed from the positive semi-definite structure tensor τ_ρ as

$$\tau_\rho(\nabla u_\sigma) := K_\rho * (\nabla u_\sigma \cdot \nabla u_\sigma{}^\perp), \quad \rho > 0 \qquad (2.4)$$

where K_ρ and K_σ denote Gaussian kernels with variance ρ and σ, respectively. u_σ is obtained convolving the fingerprint image u with K_σ. The structure tensor has two orthonormal eigenvectors

$$
\begin{aligned}
& v_1 \big\| \nabla u_\sigma \\
& v_2 \big\| \nabla u_\sigma{}^{\perp}
\end{aligned}
$$

(2.5)

The two eigenvalues λ_1, λ_2 are computed as

$$
\lambda_1 = \frac{1}{2}\left(j_{11} + j_{22} + \sqrt{(j_{11} - j_{22})^2 + 4j_{12}{}^2} \right)
$$
$$
\lambda_2 = \frac{1}{2}\left(j_{11} + j_{22} - \sqrt{(j_{11} - j_{22})^2 + 4j_{12}{}^2} \right)
$$

where

$$
j_{11} = K_\rho * \left(\frac{\partial}{\partial x} u_\sigma \right)^2
$$

(2.6)

$$
j_{12} = j_{21} = K_\rho * \left(\frac{\partial}{\partial x} u_\sigma \frac{\partial}{\partial y} u_\sigma \right)
$$

$$
j_{22} = K_\rho * \left(\frac{\partial}{\partial y} u_\sigma \right)^2
$$

The solution of (2.3) by numerical technique gives an enhanced fingerprint image resulting from the diffusion filtering process.

2.8 Short Time Fourier Transform (STFT)

The short time Fourier transform (STFT) is useful for analyzing non-stationary signals. The local ridge orientation and ridge frequency vary slowly throughout the fingerprint image. Therefore, the fingerprint image may be considered as a non-stationary signal and STFT analysis may be applied for its decomposition. To perform STFT

analysis, a window function of finite length needs to be chosen. The fingerprint image is truncated using the selected window at t=0. The truncated image is then transformed to obtain frequency spectrums using the Fourier transform. This process continues until the window covers the entire image. The STFT of one-dimensional signal (1-D) as x(t) can be represented by [10]

$$X(\tau,\omega) = \int_{-\infty}^{\infty} x(t)\omega^*(t-\tau)e^{-j\omega t}dt \qquad (2.7)$$

The STFT for a two-dimensional (2-D) signal, such as fingerprint image, can be represented by [10]

$$X(\tau_1,\tau_2,\omega_1,\omega_2) = \int_{-\infty}^{\infty}\int_{-\infty}^{\infty} I(x,y)W^*(x-\tau_1,y-\tau_2)e^{-j(\omega_1 x+\omega_2 y)}dxdy \quad (2.8)$$

where τ_1, τ_2 represent the spatial position of the 2-D window $W(x, y)$ and ω_1, ω_1 represent the spatial frequency parameters.

2.9 Summary

In this chapter, the background material necessary for the development of a fingerprint enhancement technique has been presented. Two types of fingerprint recognition systems, namely verification and identification, have been discussed in detail. Next, the important features of fingerprint image, namely, global and local features used in the feature extraction and matching stages of a fingerprint recognition have been described. The most important metrics in terms of quality, complexity and recognition rate used to measure the performance of the work undertaken in this thesis have been

presented. The databases to be used to perform different experiments on fingerprint have also been discussed.

Since the objective of the work undertaken in this thesis is to develop a method for the enhancement of the quality of a fingerprint image by filtering techniques in both spatial and frequency domain, an anisotropic diffusion filter driven by the image gradients is discussed for filtering in the spatial domain. And, we have also described short time Fourier transform (STFT) in order to perform filtering in the frequency domain.

Chapter 3

A Three-stage Scheme for Fingerprint Image Enhancement

3.1 Introduction

Availability of a good-quality fingerprint image is essential for feature extraction and matching in a fingerprint recognition system. A low-quality fingerprint image consisting of broken ridges, scars, smears, creases and falsely conglutinated ridges, has to be enhanced to improve the quality of the fingerprint image.

In this chapter, we propose a novel and effective three-stage enhancement algorithm to enhance the quality of fingerprint images. The proposed enhancement scheme is illustrated by the block diagram of Figure 3.1. The first-stage consists of a linear anisotropic diffusion filter steered by a diffusion tensor obtained from a precomputed orientation field (OF) to connect the broken ridges. In the second stage, a compensation filter is applied to the enhanced image from the first stage to improve and overcome the shortcomings of the first stage. The third stage consists of an angular filter to overcome the shortcomings of the second-stage filter that enhances the quality of fingerprint images further.

In Section 3.2, the most recent enhancement scheme using a diffusion filter [8] is studied and its limitations provided, in order to propose a simple and computation-efficient first stage filter. A detailed and systematic development of the first stage enhancement scheme using a linear anisotropic diffusion filter, as well as a technique for estimating the orientation field, is carried out in Section 3.3. To overcome the

shortcomings of the first stage filter, a second stage enhancement is proposed in Section 3.4. The development of spectral window to drive the third stage filter is discussed in detail in Section 3.5. In Section 3.6, subjective and objective results of enhanced fingerprint images obtained by applying the proposed technique to a number of databases are provided and these results are compared with those obtained by using some existing schemes. Finally, in Section 3.7, the work presented in this chapter is summarized and some of the important attributes of the proposed method highlighted.
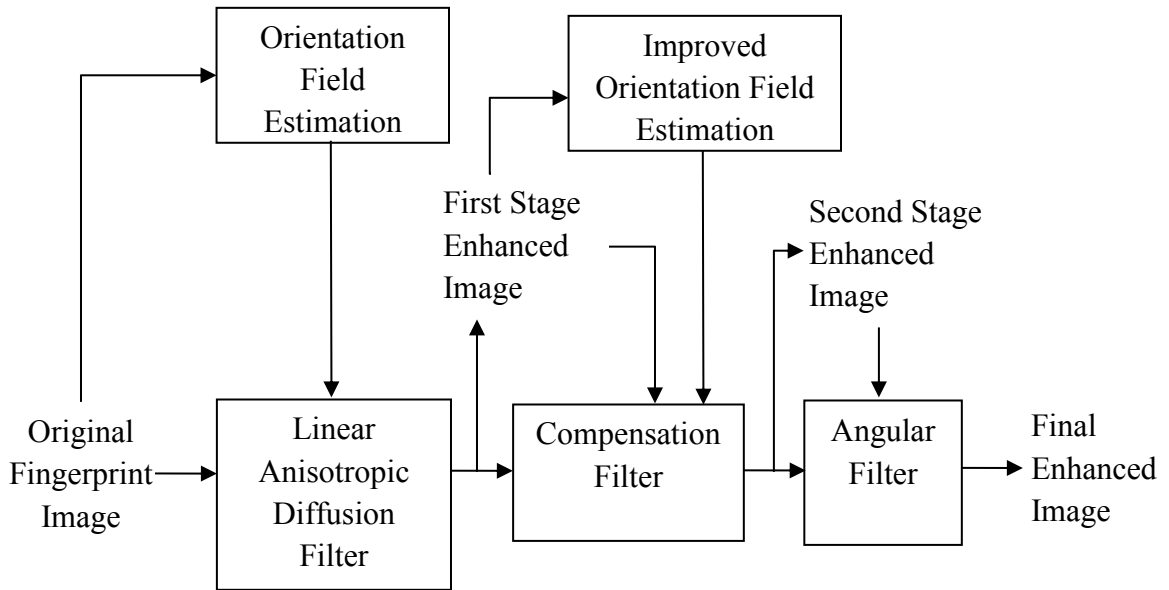
Figure 3.1 Proposed three-stage enhancement scheme.

3.2 Anisotropic Diffusion Filtering based on Orientation Field

There are several methods to enhance fingerprint images based on diffusion filtering technique [6-8, 26]. The enhancement schemes based on diffusion process in the literature could be categorized into three groups: 1) Enhancement schemes based on the gradient, 2) Orientation field-based enhancement schemes, and 3) singularity driven diffusion schemes. In this section, a fingerprint enhancement method based on a

combination of first two schemes [8] is reviewed and its drawbacks are described. As mentioned in Chapter 2, the OF plays a very important role in a fingerprint recognition system. Some researchers have used the OF for the enhancement of a fingerprint image. In [8], Gottschlich and Schönlieb have proposed an enhancement technique based on an iterative diffusion filter by driving the diffusion tensor with gradient and a precomputed orientation field. This scheme starts by computing a pixelwise OF using two orientation estimation methods, line sensor based method [37] and the gradient based method [38-39], for the input fingerprint image. The two computed OFs are compared and the final OF obtained based on a threshold, t. If the angle between the two estimations is lower than the threshold (t=15^0), the final OF is the average of the two for that pixel; otherwise the final OF is the same as the one computed by the line sensor method [37]. This OF is fed to the diffusion tensor as input to drive the filtering process with forty iterations, followed by a locally adaptive contrast enhancement step.

The main drawback associated with the above fingerprint enhancement scheme is its dependency on an accurate orientation field computation from the input fingerprint image. Although the degradation of contrast in the enhanced image after diffusion is recovered using a locally adaptive contrast enhancement stage, the improvement in contrast is not adequately achieved. In addition, the method suffers from high computation cost because of the large number of iterations required and estimation of an accurate orientation field.

3.3 Proposed First-stage Enhancement

Based on the discussion in the previous section, we can draw two main observations: 1) an accurate estimation of the orientation field and iterative diffusion result in a high computational complexity, and 2) the contrast is affected due to the iterative process of diffusion. Therefore, we now aim at developing a new fingerprint enhancement method that is based on a diffusion filter with a simple estimation of OF and a small number of iterations.

In the proposed first-stage enhancement, the original fingerprint image is enhanced with a linear anisotropic diffusion filter based on the image gradient and a simple estimation of the OF. The OF is computed from a gradient-based estimation method and the filtering process is performed with a small number of iterations. This makes the proposed first stage enhancement faster than the scheme in [8]. A block diagram of the first stage enhancement is shown in Figure 3.2.
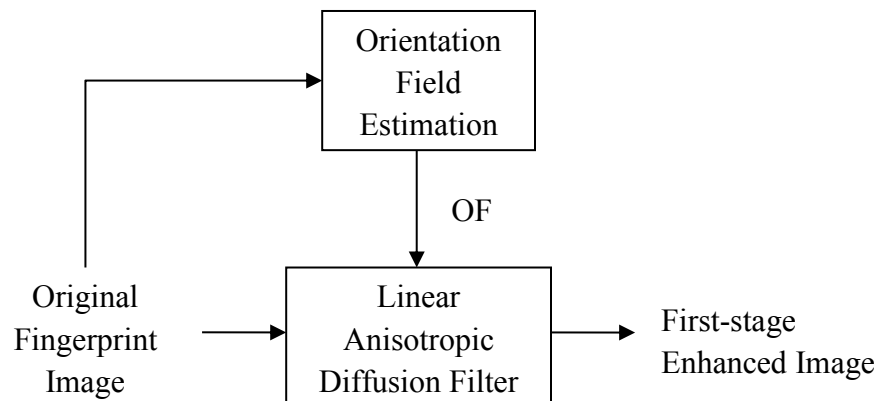
Figure 3.2 Block diagram of first-stage enhancement.

To start with, the diffusion tensor (D) of the fingerprint image is derived by a method similar to that proposed by Gottschlich and Schönlieb [8]. The diffusion tensor consists of a structure tensor (τ_ρ) and eigenvalues λ_1 and λ_2. The structure tensor is computed from the proposed estimation of the OF by computing the gradients of the OF thus allowing the diffusion tensor to be dependent not only on the gradients, but also on OF. The two eigenvalues λ_1 and λ_2 represent the diffusivities in the eigenvectors, v_1 and v_2, parallel to the two orthogonal directions given by OF. Then, the linear anisotropic diffusion filter is driven by the computed diffusion tensor. The first stage enhanced image is obtained by applying the diffusion filter with an explicit time stepping scheme.

As mentioned previously, the estimation of OF in [8] is based on two methods that increases the computational complexity of the diffusion filtering enhancement scheme. In order to reduce the computational complexity of the oriented linear anisotropic diffusion filter, we propose in the following section a simple method for estimating OF based on gradients.

3.3.1 Proposed Orientation Field Estimation

To start with, OF of the original fingerprint image is obtained by a method similar to that proposed by Ratha et al [33]. The original FP image is divided into nonoverlapping blocks of size $W \times W$. A single orientation is assigned corresponding to the dominant orientation of the block. The block orientation values are calculated using vertical and horizontal gradients of the fingerprint image by applying a simple gradient operator.

There are several gradient operators, such as Sobel, Prewitt, Robert, and Marr-Hildreth to compute image gradients. The gradient operator is generally selected depending on the computational requirement. The most used gradient operator is a Sobel mask to compute OF of the fingerprint image [33]. A 3×3 Sobel operator is shown in Figure 3.3. The Sobel mask is less susceptible to noise, but it produces thicker edges. Therefore, a Gaussian mask rather than traditional Sobel mask is applied for the gradient computation to estimate OF of the original fingerprint image for the proposed first-stage enhancement. Some examples of the Gaussian operator are shown in Figures 3.4 and 3.5.

The proposed first stage enhancement is summarized in Algorithm 3.1.

+1	0	-1
+2	0	-2
+1	0	-1

+1	+2	+1
0	0	0
-1	-2	-1

(a)   (b)

Figure 3.3 3×3 Sobel operators to compute (a) horizontal gradients and (b) vertical gradients.

0.0725	0	-0.0725
0.5355	0	-0.5355
0.0725	0	-0.0725

0.0725	0.5355	0.0725
0	0	0
-0.0725	-0.5355	-0.0725

(a)   (b)

Figure 3.4 3×3 Gaussian operators to compute (i) horizontal gradients, (ii) vertical gradients.

Finally, the orientation field is multiplied by a factor to estimate OF of the original fingerprint image more accurately. The multiplying factor is determined empirically and the range varies from 0.1 to 0.35. This orientation field indicated in Figure 3.2 is the precomputed OF. The diffusion tensor of the oriented linear anisotropic diffusion filter is driven by OF to perform the first stage enhancement.

0.0002	0.0005	0.0008	0	-0.0008	-0.0005	-0.0002
0.0027	0.0064	0.0093	0	-0.0093	-0.0064	-0.0027
0.0120	0.0288	0.0418	0	-0.0418	-0.0288	-0.0120
0.0198	0.0474	0.0688	0	-0.0688	-0.0474	-0.0198
0.0120	0.0288	0.0418	0	-0.0418	-0.0288	-0.0120
0.0027	0.0064	0.0093	0	-0.0093	-0.0064	-0.0027
0.0002	0.0005	0.0008	0	-0.0008	-0.0005	-0.0002

(a)

0.0002	0.0027	0.0120	0.0198	0.0120	0.0027	0.0002
0.0005	0.0064	0.0288	0.0474	0.0288	0.0064	0.0005
0.0008	0.0093	0.0418	0.0688	0.0418	0.0093	0.0008
0	0	0	0	0	0	0
-0.0008	-0.0093	-0.0418	-0.0688	-0.0418	-0.0093	-0.0008
-0.0005	-0.0064	-0.0288	-0.0474	-0.0288	-0.0064	-0.0005
-0.0002	-0.0027	-0.0120	-0.0198	-0.0120	-0.0027	-0.0002

(b)

Figure 3.5 7×7 Gaussian operators to compute (i) horizontal gradients, (ii) vertical gradients.

Algorithm 3.1: First stage Enhancement with Linear Anisotropic Diffusion Filter

1. Divide the input fingerprint image ($M \times N$ pixels) into $W \times W$ blocks.

2. For each pixel in a block, compute the horizontal gradients (G_x) and vertical gradient (G_y) by applying the 7×7 Gaussian gradient operator.

3. Compute the dominant ridge of the block using

$$O(i,j) = \frac{1}{2}\tan^{-1}\left(\frac{\displaystyle\sum_{u=i-\frac{W}{2}}^{i+\frac{W}{2}}\sum_{v=j-\frac{W}{2}}^{j+\frac{W}{2}}2G_x(u,v)G_y(u,v)}{\displaystyle\sum_{u=i-\frac{W}{2}}^{i+\frac{W}{2}}\sum_{v=j-\frac{W}{2}}^{j+\frac{W}{2}}G_x^{\ 2}(u,v)G_y^{\ 2}(u,v)}\right) \tag{3.1}$$

4. Determine the precomputed OF, $O_{PC}(i, j)$, from the orientation field obtained in the previous step, by multiplying it with a factor, M_P of 0.25.

$$O_{PC}(i,j) = O(i,j) \times M_P (= 0.25) \tag{3.2}$$

5. Apply linear anisotropic diffusion filter to the original fingerprint image, $I(x,y)$ using the equation:

$$\begin{cases} \dfrac{\partial u}{\partial t} = div(D(\tau_\rho(\nabla u_\sigma), O_{PC})\nabla u) & on\ \Omega \times (0,\infty) \\ u(x,y,0) = I(x,y) & on\ \Omega \\ \left\langle D(\tau_\rho(\nabla u_\sigma), O_{PC})\nabla u, n\right\rangle = 0 & on\ \partial\Omega \times (0,\infty) \end{cases} \tag{3.3}$$

where u is filtered or first stage enhanced image, D is diffusion tensor, τ_ρ is structure tensor, and **n** is the outward pointing unit normal vector on $\partial\Omega$.

6. Compute the structure tensor from the precomputed OF, $O_{PC}(i, j)$ by

$$S(G) = \begin{bmatrix} s_{11} & s_{12} \\ s_{21} & s_{22} \end{bmatrix} = \begin{bmatrix} G_x \times G_x & G_x \times G_y \\ G_y \times G_x & G_y \times G_y \end{bmatrix}$$ (3.4)

where G_x and G_y are the gradients estimated from O_{PC}.

- Choose the eigen values to build the diffusion tensor D as

$$\lambda_1 = a,$$
$$\lambda_2 = \begin{cases} a, & \text{if orientation could not be estimated in } I(x,y) \\ 1, & \text{if orientation could be estimated in } I(x,y) \end{cases}$$ (3.5)

where a denotes strength of diffusion and $I(x, y)$ is the original fingerprint image.

- Compute diffusion tensor, D using the equation

$$D(S) = \begin{bmatrix} \lambda_1 + \lambda_2 + [(\lambda_2 - \lambda_1) \times (s11 - s22)/a] & (\lambda_2 - \lambda_1) \times s12/a \\ (\lambda_2 - \lambda_1) \times s12/a & \lambda_1 + \lambda_2 - [(\lambda_2 - \lambda_1) \times (s11 - s22)/a] \end{bmatrix}$$ (3.6)

- Finally, the first-stage enhanced image, I_{FT} is obtained by the explicit time stepping scheme with iterations as

$$I_{FT} = u(x, y, t+T) = u(x, y, t) + T \times \frac{du}{dt}$$ (3.7)

where T is the step size.

In order to show the effectiveness of the proposed first stage enhancement, two experiments are conducted. In the first one, a fingerprint image from the FVC2004 (DB1A) database, consisting of broken ridges is enhanced using the proposed Algorithm 3.1. Figure 3.6 shows the original image along with its enhanced images using the Sobel and Gaussian gradient operators. It is observed from the enhanced images that the Gaussian gradient operator yields results better than that obtained by using the Sobel

operator in enhancing the fingerprint image near singular points and boundaries of the fingerprint for the oriented linear anisotropic diffusion filter. The arrow and circle at boundaries and near singular point regions, respectively, show that the Gaussian gradient operator overcomes the limitations of the Sobel operator successfully in enhancing the fingerprint image.

In the second experiment, the same fingerprint image from FVC2004 (DB1A) database is enhanced using the proposed first stage algorithm (Algorithm 3.1) by varying the value of the multiplying factor M_P. The effects of without and with multiplying factors in the first-stage enhanced images are observed in Figure 3.7. It is seen that the enhanced image without M_P (Figure 3.7 (a)) contains blurred regions indicating poor enhancement. It is also observed that the lower and higher values than 0.25 could not enhance the fingerprint image as shown in Figures 3.7(b-e). It is seen that the enhanced image (Fig 3.7 (f)) with $M_P = 0.25$ gives the best enhancement result.

From the two experiments, it is seen that fingerprint images consisting of broken ridges could be enhanced using the proposed first stage enhancement algorithm with a Gaussian operator and a multiplying factor of value 0.25. The filtering process is an iterative one and number of iterations used is ten. A small number of iterations is used in order to keep the computational complexity of the proposed algorithm. In Figure 3.8, more enhanced images are shown using the proposed first stage scheme from different sub-databases (i.e., FVC2004:DB2A, DB3A and DB4A).

Figure 3.6 (a) Original image. The first-stage enhanced image using
(b) Sobel and (c) Gaussian masks with $M_P = 0.25$.
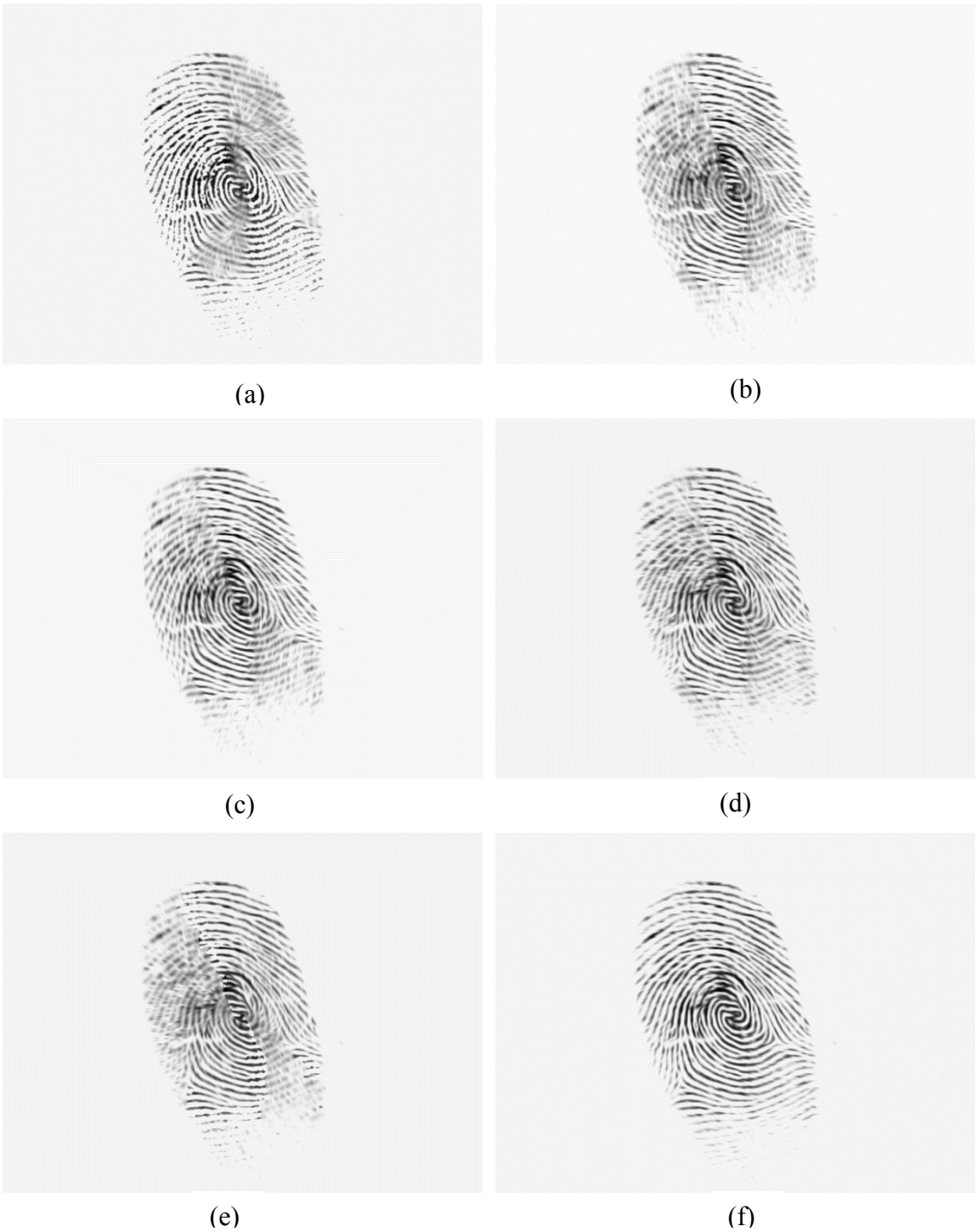
Figure 3.7 First stage enhanced images with Gaussian gradient operator and different
values of the (a) $M_P = 1.0$, (b) $M_P = 0.1$, (c) $M_P = 0.15$, (d) $M_P = 0.3$, (e) $M_P = 0.35$ and (f) $M_P = 0.25$.

(a)   (b)   (c)

(d)   (e)   (f)
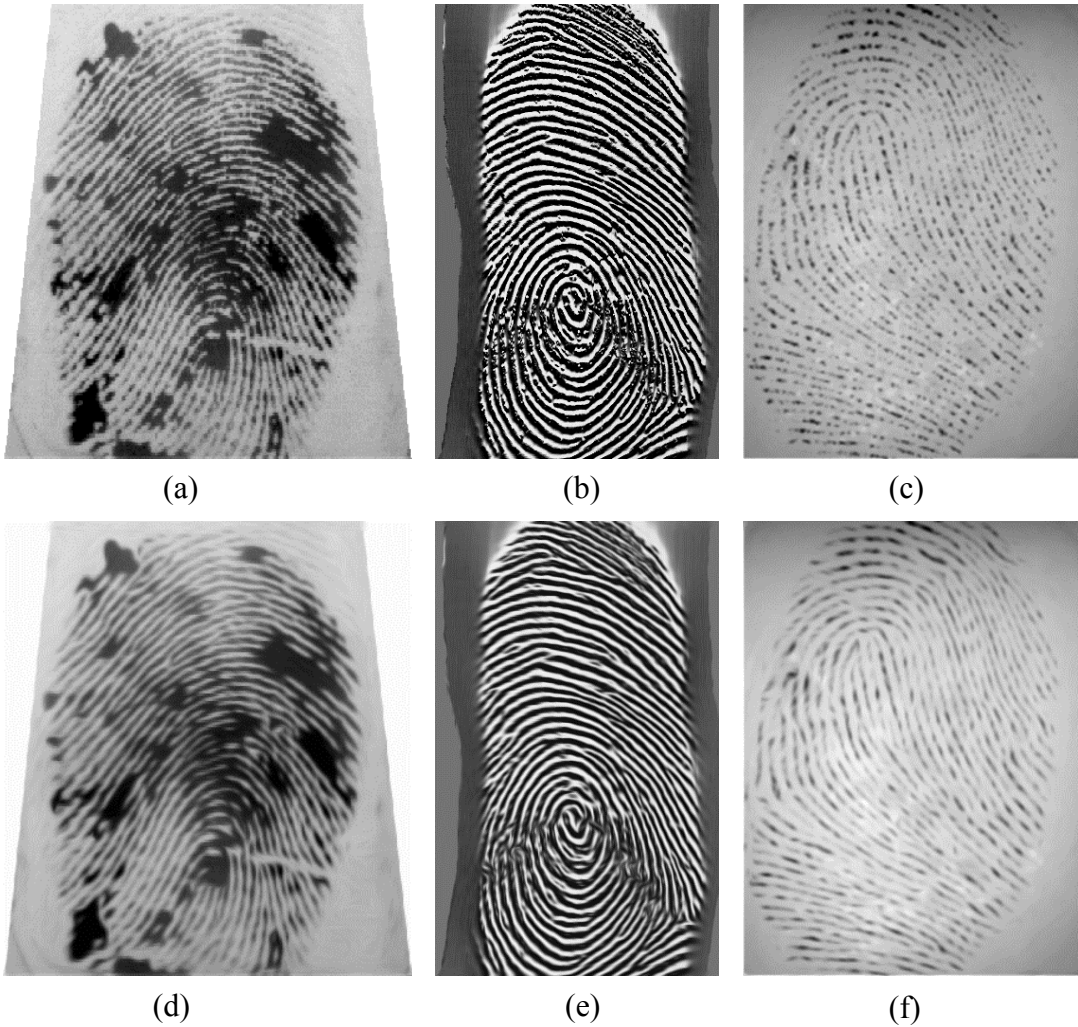
Figure 3.8 Some other examples of enhancing fingerprint images from the FVC2004 by
applying Algorithm 3.1 with $M_P = 0.25$. Original images (a) DB2A, (b)
DB3A, (c) DB4A. (d)-(f) The corresponding enhanced images.

Although the proposed first stage filter improves the quality of the original fingerprint images shown in Figures 3.6 (a) and 3.8 (a), it cannot join broken ridges created by scars or creases after the first stage enhancement as illustrated in Figures 3.6 (c) and 3.8 (d), respectively.

Hence, the objective to connect broken ridges is only partially fulfilled after the first-stage enhancement. It should also be noticed that the contrast of the enhanced image

is degraded due to the number of iterations applied during the linear anisotropic diffusion filtering process. Also, the first stage has a limitation in adequately enhancing an image if the original image has parallel ridges that are not well separated or has smears (Figure 3.8 (a)). In the next section, we propose another stage of enhancement to overcome the shortcomings of the first-stage.

3.4 Proposed Second-stage Enhancement

The linear anisotropic diffusion filter presented as the first-stage of the proposed enhancement scheme in the previous section, was designed to connect broken ridges of fingerprint images. But, the broken ridges due to scars and creases still remain in the enhanced images; in addition, some contrast degradation of the fingerprint image is noted after the first-stage enhancement. Also, it cannot recover the regions covered by smears and separate some falsely connected ridges. Therefore, a second stage filter is introduced to connect the broken ridges completely and improve the contrast of the images obtained after the first-stage enhancement, as well as to overcome the other limitations of this stage. To perform the second-stage enhancement, an effective compensation filter as in [15], is applied. The ridge compensation filter in [15] is computationally complex due to the necessity of applying a large number of iterations. In addition, the estimation of the orientation field to drive the compensation filter is based on the Sobel gradient operator, which is less effective as mentioned in Section 3.3.1. Therefore, for the second-stage enhancement, an oriented ridge compensation filter, performing without iterations, is proposed. The second-stage filter is driven by the orientation field estimation proposed in Section 3.3.1.

The proposed second-stage enhancement is illustrated by the block diagram of Figure 3.9. At first, the input image (first-stage enhanced image) is divided into nonoverlapping blocks. In order to adjust the gray level deformation in the fingerprint image, a local normalization is carried out for each block. Then, the OF is estimated from the normalized image using an approach similar to that in Section 3.3.1. The OF of the original fingerprint image was accurately estimated using a multiplying factor in the first-stage enhancement. Hence, OF in this stage is estimated without the use of the multiplying factor M_P. In the final step, the normalized image is filtered with the local ridge compensation filter oriented along the ridge direction.

First-stage
Enhanced
Image

| Local Normalization | Improved Orientation Field Estimation | Compensation Filter |

Second-stage
Enhanced
Image
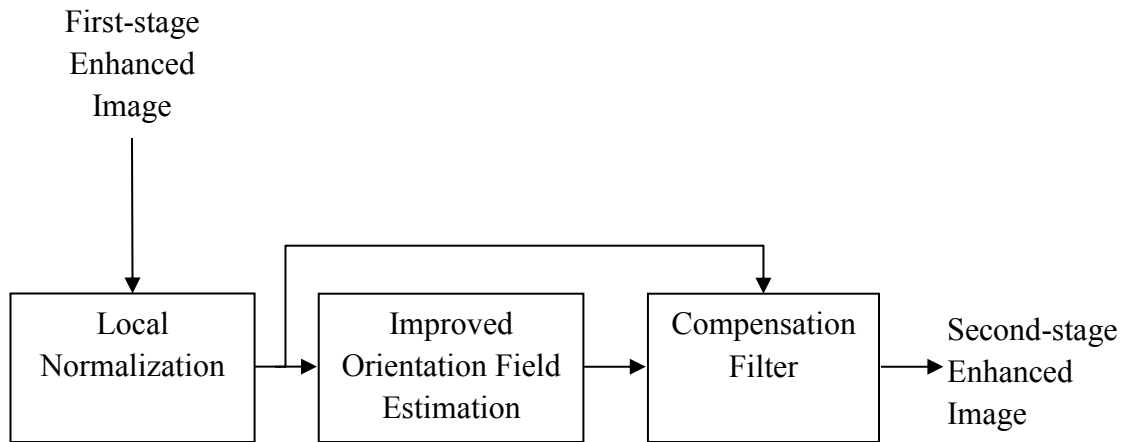
Figure 3.9 Block diagram of the second-stage enhancement.

The proposed second-stage enhancement described in the preceding paragraphs is now be summarized as an algorithm (Algorithm 3.2).

Algorithm 3.2: Second-stage Enhancement with Oriented Local Ridge Compensation Filter

1. Divide the first-stage enhanced fingerprint image, $I_{FT}(i,j)$ into $W{\times}W$ nonoverlapping blocks.

2. Perform local normalization at each pixel of the blocks as

$$N(i,j) = M_0 + \frac{V_0}{V} \times \left(I_{FT}(i,j) - M\right) \qquad (3.8)$$

where N is the normalized image at pixel (i,j), M and V are the block mean and variance, respectively, and M_0 and V_0 are the desired mean and variance for all blocks, respectively.

3. Compute the improved orientation field, $O_I(i,j)$ from the normalized image similar to Section 3.3.1 excluding the multiplying factor.

4. Apply the ridge compensation filter to the normalized image to obtain the second-stage enhanced image by using the following equations:

$$I_{ST}(i,j) = \frac{\left(\displaystyle\sum_{m=-(w-1)/2}^{(w-1)/2} \sum_{n=-(h-1)/2}^{(h-1)/2} N(i',j')\right)}{(((w-1)\times\beta+\alpha)\times h)}$$
$$i' = i + m\cos(O_I(i,j)) + n\sin(O_I(i,j)) \qquad (3.9)$$
$$j' = j - m\sin(O_I(i,j)) + n\cos(O_I(i,j))$$

where m and n are the locations of filter mask of size $w{\times}h$. α and β are contrast parameters and (i',j') is the new axes of pixel coordinate to make the ridge compensation filter oriented along the local ridge direction.

The values of the parameters for local ridge compensation filter are chosen to be the same as in [15] except for the number of iterations applied. The computation time in

the spatial domain depends on the size of the mask as well as the number of iterations. The proposed second-stage filter is faster than the ridge compensation filter in [15] due to the characteristic of non-iterative filtering process.

In order to show the usefulness of the proposed second-stage enhancement, two experiments are conducted. In the first one, the original fingerprint image from the database FVC2004 (DB1A) consisting broken ridges and scars, is enhanced using the proposed first and second-stage filters. Figure 3.10(a) shows the original fingerprint image and Figures 3.10 (b) and (c) the images after the first- and second-stage enhancements. By comparing Figures 3.10 (b) and (c), two main observations can be made. First, the ridges broken due to scars/creases (indicated by a square) are successfully joined in the latter. Second, the contrast is improved to a large extent in the enhanced image of (c). These two observations show that second stage enhancement completely connects the broken ridges and effectively improves the contrast of the fingerprint images.

In the second experiment, the fingerprint image from the database FVC2004 (DB2A) consisting of smears and falsely connected ridges, is enhanced using the proposed first and second-stage filters. Figure 3.11(a) shows the original fingerprint image and Figures 3.11 (b) and (c) its enhanced versions. By comparing the enhanced images in Figures 3.11(b) and (c), two main observations can be made. First, the falsely conglutinated ridges are separated (indicated by square) successfully in the latter. Second, the smears are removed as indicated by arrows in Fig 3.11(c).These two observations suggest that second-stage enhancement separates falsely connected ridges as well as it removes smears in fingerprint images. However, there are still some other ridges that

44

Figure 3.10 (a) An original FVC2004 (DB1A) fingerprint image. Enhanced fingerprint images after the (b) first-stage processing, and (c) second-stage processing.

(a)   (b)   (c)
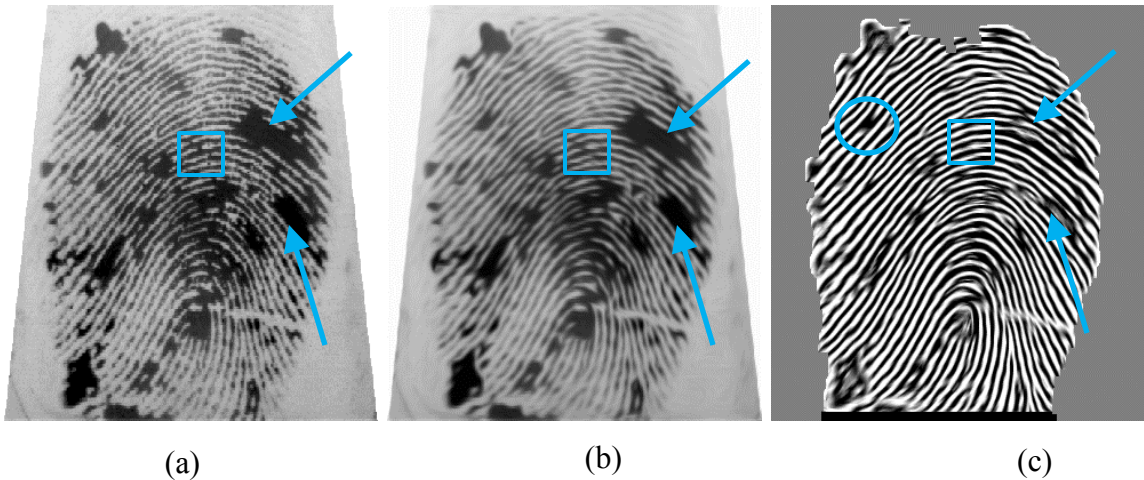
Figure 3.11 (a) An original FVC2004 (DB2A) image, (b) First-stage enhanced image,
(c) Enhanced image after two stages.

need to be separated, as indicated in Fig 3.11(c) by circles. Also, the removal of smears is not fully satisfactory as indicated by the arrows in the same figure. It should also be noticed that there is an unexpected black region that appears at the bottom border of the enhanced image.

From the two experiments performed above it is clear that the images consisting of broken ridges and scars/creases (e.g., those from FVC2004 (DB1A) could be enhanced effectively using the proposed second stage filter. However, the fingerprint images of poor quality such as FVC2004(DB2A) require further filtering in order to fully separate falsely connected ridges as well as to remove smears and unexpected borders efficiently. In the following section, a third-stage enhancement scheme is proposed in order to address the shortcomings of the second-stage and to improve the quality of the fingerprint images in all databases.

3.5 Proposed Third-stage Enhancement

Based on the discussion in the previous section, a third-stage enhancement is performed to overcome the limitations of the second stage. In the proposed third-stage enhancement, the fingerprint image obtained from the second stage filter is further enhanced with an angular filter based on Gaussian function. The third stage enhancement consists of two phases: 1) STFT analysis and 2) enhancement by angular filter as shown in Fig 3.12.

Second-stage
Enhanced
Image

| Short Time Fourier Transform (STFT) | → | Angular Filter | → | Third-stage/Final Enhanced Image |
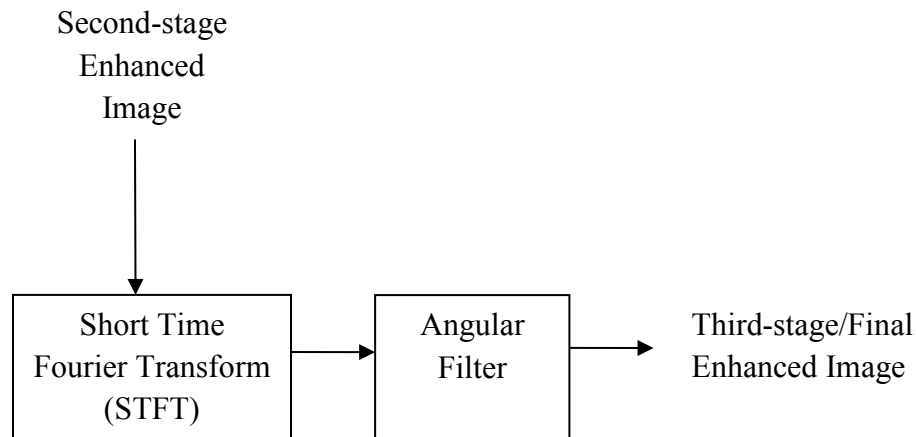
Figure 3.12 Block diagram of third-stage enhancement.

In the first phase, the short time Fourier transform (STFT) is performed using Gaussian spectral window. The second-stage enhanced fingerprint image, $I_{ST}(i,j)$ is divided into overlapped blocks. The block images are multiplied by a spectral window, $W(i,j)$. Since the third-stage enhancement consists of overlapped block processing image operations, the blocking effect may be visible in the enhanced image if it is not taken appropriately. This blocking effect may be controlled by choosing an appropriate spectral window for the STFT analysis. There are several spectral windows, such as hanning,

hamming or raised cosine window, that can be used to perform STFT analysis. The most popular spectral window used in fingerprint image enhancement is the raised cosine window used by Chikkerur et al. [10]. However, we choose the Gaussian spectral window rather than the raised cosine window, since the Fourier transform or the derivative of a Gaussian function is also Gaussian. In STFT analysis, the Gaussian spectral window used can be defined by

$$W(i,j) = \begin{cases} 1 & \text{if } (|i|,|j| < BLKSZ/2) \\ \exp\left(\dfrac{-0.5*i}{WNDSZ/2}\right) & \text{otherwise} \end{cases} \quad (i,j) \in \left(-\dfrac{WNDSZ}{2}, \dfrac{WNDSZ}{2}\right) \quad (3.10)$$

where BLKSZ is the block size, OVRLP is the overlap of the window, and WNDSZ is the window size. This spectral window puts more weight at the center of the window and less at the edges as shown in Figure 3.13. The weight of the Gaussian window from center to the edges reduces with small deviations, thus makes it better than the raised cosine window. The red and blue colors indicate the highest and lowest values of the spectral window, respectively. Then, the fast Fourier transform (FFT) of each block is obtained followed by a simple root filtering. The ridge orientation field, $E\{\theta\}$ is approximated probabilistically for each block and smoothened by a Gaussian kernel to obtain a more accurate orientation field, $O_{TS}(i,j)$. The coherence image, $C(i,j)$ is then computed using $O_{TS}(i,j)$.

In the second phase, each block is enhanced using an angular filter, which is a Gaussian filter in the frequency domain. The orientation field and the coherence image obtained from the STFT analysis are used to design the angular filter. This filter is centered at $O_{TS}(i,j)$ and the bandwidth is inversely proportional to $C(i,j)$. Then, this

angular filter is applied on each block FFT to obtain enhanced blocks in frequency domain. The enhanced fingerprint image is reconstructed combining all the block enhanced images. Finally, a segmentation method based on morphological operation [37] is applied to segment the foreground from the background in the enhanced fingerprint image.
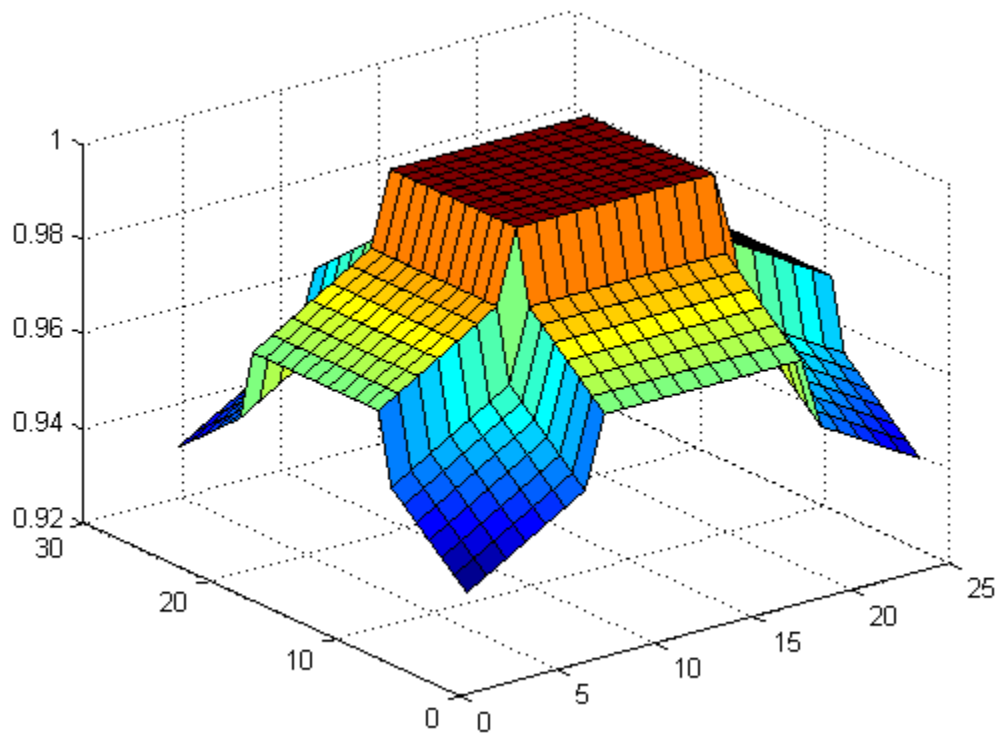
Figure 3.13 Spectral window used for STFT analysis.

The proposed third-stage enhancement described in the preceding paragraphs can now be summarized as Algorithm 3.3 below.

Algorithm 3.3: Third-stage Enhancement with an Angular Filter

Phase-1: STFT Analysis

1. Divide the second-stage enhanced fingerprint image, $I_{ST}(i,j)$ into $N \times N$ overlapping blocks, $I_B(i,j)$.

2. Remove the DC content of $I_B(i,j)$ as

$$I_B(i,j)= I_B(i,j)\text{-}avg(I_B(i,j)) \tag{3.11}$$

3. Multiply each of the overlapping blocks by the proposed Gaussian spectral window W, as

$$I_B(i,j) = I_B(i,j) \times W(i,j) \tag{3.12}$$

4. Apply FFT on each block to obtain block FFT $I_{BFFT}(\omega_1, \omega_2) = \text{FFT}(I_B(i,j))$.

5. Perform root filtering on $I_{BFFT}(\omega_1, \omega_2)$.

6. Compute the orientation field, $E\{\theta\}$ using the probabilistic approximation

$$E\{\theta\} = \frac{1}{2}\tan^{-1}\left\{\frac{\left|\int_\theta p(\theta)\sin(2\theta)d\theta\right|}{\int_\theta p(\theta)\cos(2\theta)d\theta}\right\} \tag{3.13}$$

where $p(\theta)$ is the probability density function of the orientation field θ, which is a random variable.

7. The third-stage orientation field, $O_{TS}(i,j)$ is then obtained by smoothing $E\{\theta\}$ with a Gaussian kernel, $G(i,j)$ of size $K \times K$ as

$$O_{TS}(i,j) = \frac{1}{2}\tan^{-1}\left\{\frac{\sin(2E\{\theta\}*G(i,j))}{\cos(2E\{\theta\}*G(i,j))}\right\} \tag{3.14}$$

8. Compute the coherence image $C(i,j)$ to adapt the angular bandwidth of the third-stage filter as

$$C(i_0, j_0) = \frac{\sum\limits_{(x,y) \in N} \left| \cos\left(O_{TS}(i_0, j_0) - O_{TS}(i_x, j_y)\right) \right|}{N \times N} \qquad (3.15)$$

where $C(i_0,j_0)$ and $O_{TS}((i_0,j_0)$ are the coherence and orientation, respectively, at the central block, and $O_{TS}(i_x,j_y)$ is the orientation of the neighboring blocks.

Phase-2: Enhancement by Angular Filter

9. Compute the Gaussian angular filter, F_A centered around $O_{TS}(x,y)$ and the bandwidth inversely proportional to $C(x,y)$ for each overlapped block as

$$F_A(\varphi) = \begin{cases} \exp\left(-C_\varphi * \left(\dfrac{\varphi - \varphi_c}{\varphi_{BW}}\right)^2\right), & if \ |\varphi| < \varphi_{BW} \\ 0, & otherewise \end{cases} \qquad (3.16)$$

where φ_{BW} is the support and φ_C is the center of the angular filter.

10. Apply the angular filter F_A over each block to obtain the enhanced blocks in FFT domain as

$$I_{ENBFFT}(\omega_1, \omega_2) = I_{BFFT}(\omega_1, \omega_2) * F_A \qquad (3.17)$$

11. Compute the enhanced blocks, $I_{ENB}(i,j)$ in the spatial domain by inverse fast Fourier transform (IFFT) as

$$I_{ENB}(i,j) = IFFT(I_{ENBFFT}(\omega_1, \omega_2) \qquad (3.18)$$

12. The third-stage enhanced fingerprint image, $I_{TS}(i,j)$ is obtained by combining all the enhanced blocks $I_{ENB}(i,j)$.

13. Finally, a segmentation method based on morphological operation [37] is applied to segment the foreground from the background in the enhanced fingerprint image.

In order to show the effectiveness of the proposed third-stage enhancement, it is applied to the image from FVC2004 (DB2A) database. Figure 3.14(a) shows an the original image and the second and third-stage enhanced images in Fig 3.14(b and c). The original image is taken from FVC2004 (DB2A) database which consists of poor quality fingerprint images. From Fig 3.14(c), it is seen that the falsely connected parallel ridges are completely separated (marked by circle) using the third stage filter. The arrows in Fig 3.14(c) indicating the unrecovered areas due to smears in the original image shown in Fig 3.14(a) are recovered successfully after the final stage filtering. By comparing Figures 3.14(b) and (c), it can be observed that the final stage filtering overcomes all the limitations of the second stage filter.

(a)   (b)   (c)
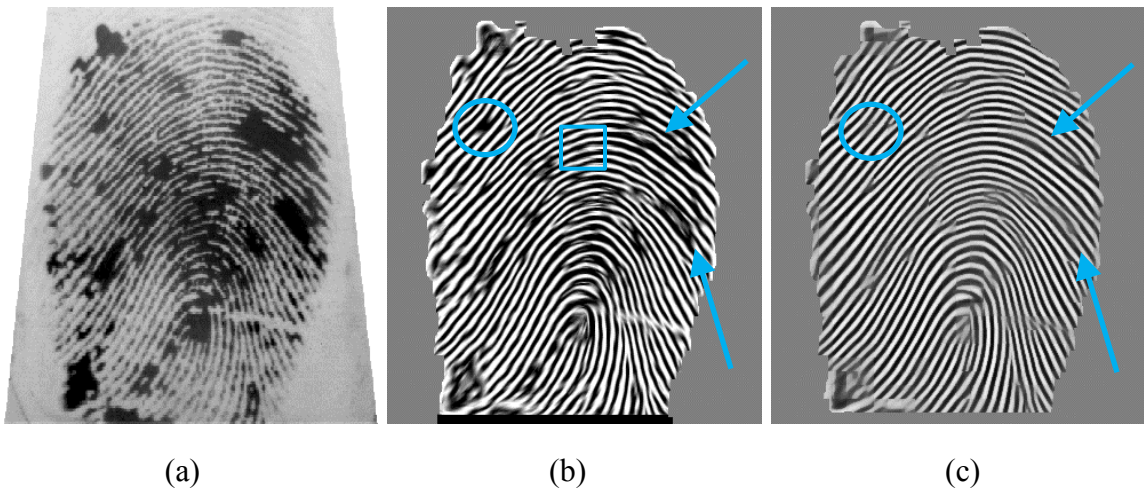
Figure 3.14 (a) An original image from FVC2004 (DB2A), (b) Second-stage enhanced image, (c) Third-stage enhanced image.

The reason for using a Gaussian window rather than a cosine one is to reduce the blocking effect during the final stage enhancement. The Gaussian spectral window is better than the cosine window in terms of reducing the blocking effect as seen in Figure 3.15. The squares indicate the blocking effects caused by the Gaussian and cosine

spectral windows in Figures 3.15 (a) and (b), respectively. The angular filter with Gaussian spectral window produces more clear regions than the raised cosine window does, as indicated by the squares in Figure 3.15.

From the output results shown in Figure 3.14, one can conclude that the quality of the fingerprint image can be enhanced if multiple stages are used. It is seen that the problems of broken ridges, scars/creases, falsely conglutinated ridges, smears and poor contrast could be dealt with effectively using the proposed three-stage enhancement scheme.

(a)   (b)
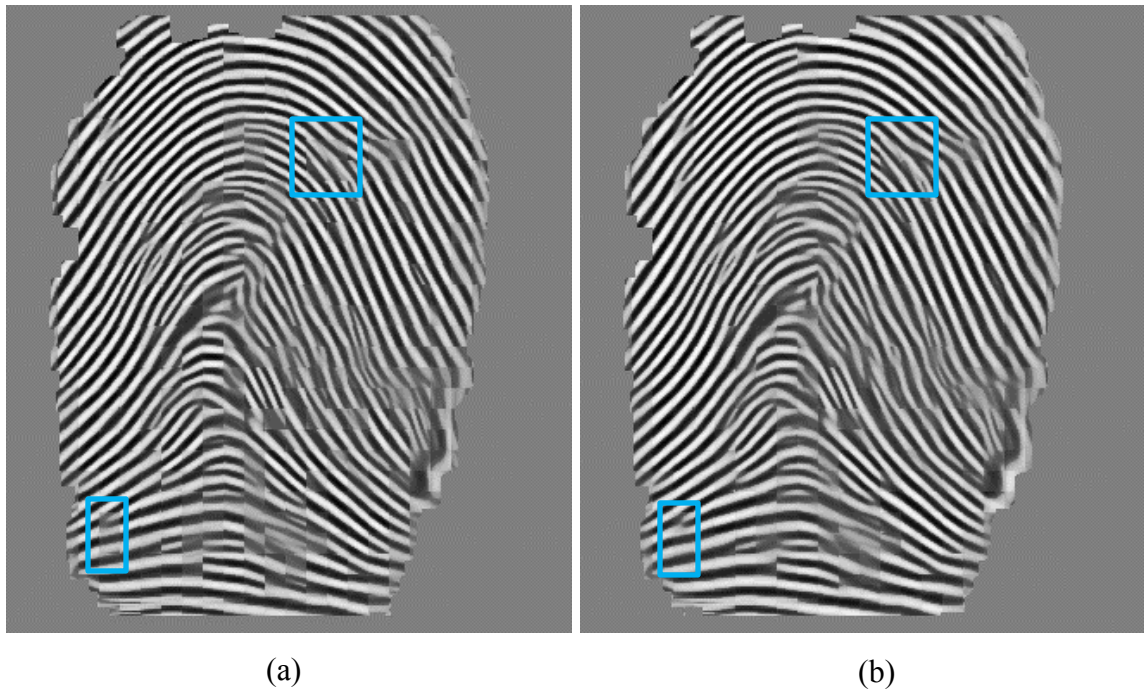
Figure 3.15 Final enhanced images using two different spectral windows in the third stage, (a) Raised cosine window and (b) Gaussian.

3.6 Performance Evaluation of the Proposed Scheme

The objective of the fingerprint image enhancement scheme presented in the previous section has been to connect broken ridges, remove scars and smears, separate conglutinated ridges and improve the contrast of fingerprint images. It is done by three stage filtering process, namely the linear anisotropic diffusion, ridge compensation and an angular filter, as explained in the previous sections. In order to assess the proposed method, we now perform experiments using the database FVC2004 (DB1A, DB2A, DB3A and DB4A). Visual as well as quantitative results using the proposed method are compared to those with two other methods presented in [8] and [15].

The performance evaluation of the proposed method is divided into two parts. In the first part, a subjective examination of MATLAB simulation results is carried out. Four images are chosen and used in the simulation. The objective measurements are presented in the second part of this section.

3.6.1 Subjective Analysis

In order to test the effectiveness of the proposed three-stage enhancement method, we conduct three experiments. In the first experiment, the proposed method is applied to the images from four different sub-databases in FVC2004, namely, DB1A, DB2A, DB3A and DB4A. Figures 3.16 - 3.19 show the simulation results obtained by applying proposed scheme on these images. In each of these figures, the original input image, the image enhanced after first, second and third stages in the simulation can be found in Appendix I.

The simulation result with the image from FVC2004 (DB1A) database is shown in Figure 3.16. The original input image consists of broken ridges as well as creases as shown in Figure 3.16(a). By means of the first stage enhancement, the broken ridges are joined as shown in Figure 3.16(b). However, one can see that the breaks created by creases still remain as well as a degradation of the contrast in the first-stage enhanced image is noticed. By applying the proposed second-stage filtering to the first stage enhanced image, one can connect small gaps created by creases along with a significant improvement in the contrast, as seen from the image in Figure 3.16(c). In Figure 3.16(d), the second-stage enhanced image is further filtered using the third stage to connect big gaps created by creases, yielding a significant improvement in the quality, as seen from the image in Figure 3.16(d). Comparison of the image in Figures 3.16(c) and (d) shows that the difference between them is only in the region of big gaps caused by creases. Therefore, one may confine using only the first two stages for fingerprint images not having this problem, for example for images from the database FVC2004 (DB1A).

The second image Figure 3.17 (a) used in the simulation, is taken from FVC2004 (DB2A) database, which is a lower quality image than that chosen from the dataset DB1A. The image has smears at different regions with broken ridges and crease. There are falsely conglutinated ridges due to smears and the contrast is poor. The result of the first, second and third stage enhancements are shown in Figure 3.17 (b), (c) and (d), respectively. Comparing the two images shown in Figures 3.17(b) and (c), one sees that the latter is better visual quality enhanced image as the second-stage removes the falsely conglutinated ridges caused by smears better than the first-stage filtering process does. However, there are more falsely connected ridges need to be recovered from the second-

stage enhanced images. By using the proposed third-stage enhancement, those falsely conglutinated ridges are recovered significantly, as seen from the image of Figure 3.17 (d). Comparing this filtered image with the original image shown in Figure 3.17(a), one can easily see the necessity of the proposed third-stage enhancement for improving the quality of the fingerprint image. In Figure 3.17(d), all the parallel ridges become clearly visible, which can hardly be seen in fingerprint images of Figures 3.17(a) and (b). The broken ridges caused by creases have been joined with a significant improvement in the contrast.

The image from FVC2004 (DB3A), as shown in Figure 3.18 (a), consists of broken ridges and noise near singular regions. By using the first-stage enhancement, the broken ridges are joined as seen in the image of Fig 3.18 (b). The enhanced image has visible noise present around the singular region. After the second-stage filtering, the noise around the singular region is removed, as seen from the image of Fig 3.18 (c). From Figure 3.18 (d), it can be seen that the final enhanced image has a much better visual quality than the original one shown in Fig 3.18(a).

Figure 3.19 (a) shows an original image taken from the database FVC2004 (DB4A), and contains broken ridges, scars and noises. The broken ridges are joined after the first-stage filtering, as seen from the image of Fig 3.19 (b). However, the visual quality is not satisfactory in some regions, which is enhanced by the second-stage filter as seen from the image of Fig 3.19 (c). Comparing the final enhanced image of Fig 3.19 (d) obtained after the third-stage filtering process with the original fingerprint image of Fig 3.19 (a), one can see that the improvement in the quality of the fingerprint image is quite significant.

(a)   (b)

(c)   (d)

Figure 3.16 (a) An original image from FVC2004 (DB1A). Enhanced images after the (b) first stage, (c) second stage and (d) third stage

(a)   (b)   (c)   (d)
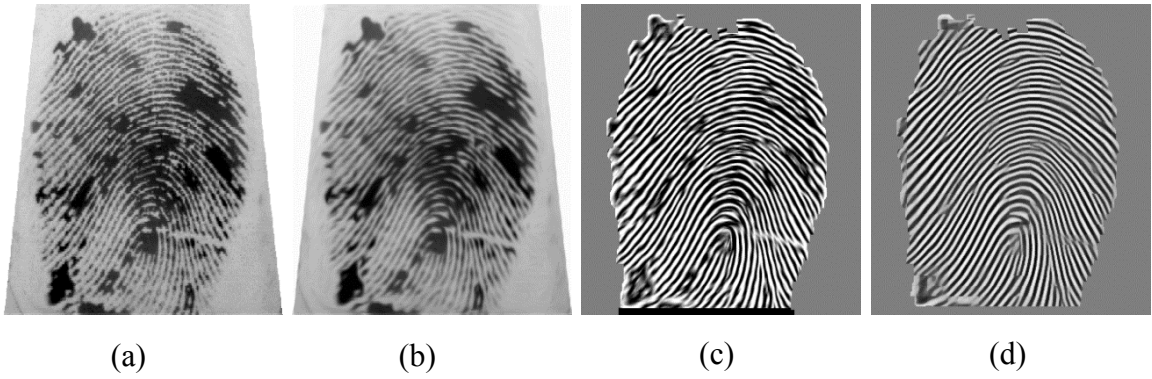
Figure 3.17 (a) Original image (FVC2004 (DB2A)), enhanced images after (b) first-stage, (c) second-stage and (d) third-stage.

(a)   (b)   (c)   (d)
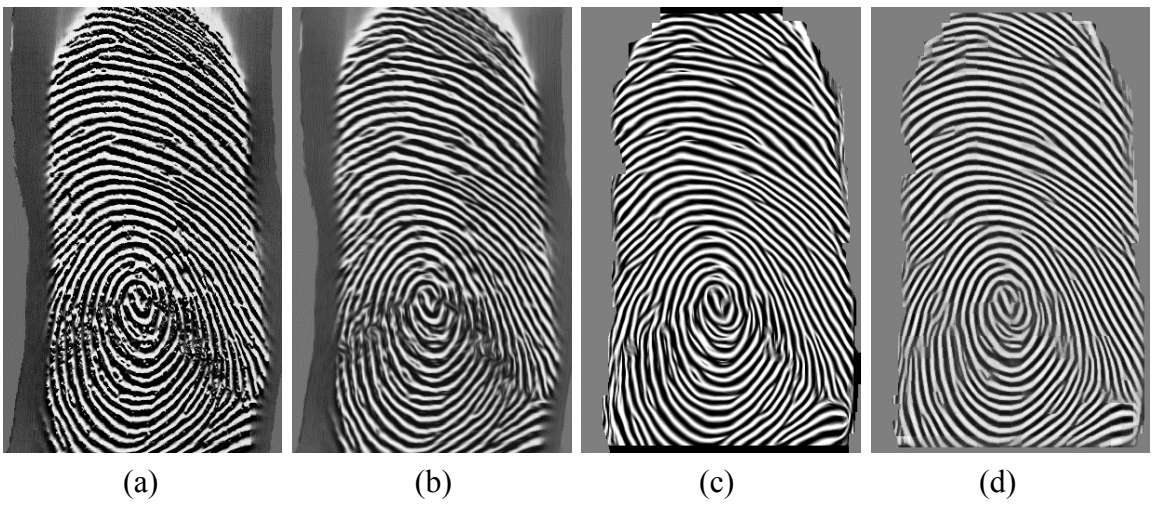
Figure 3.18 (a) Original image (FVC2004 (DB3A)), enhanced images after (b) first-stage, (c) second-stage and (d) third-stage.

(a)   (b)   (c)   (d)
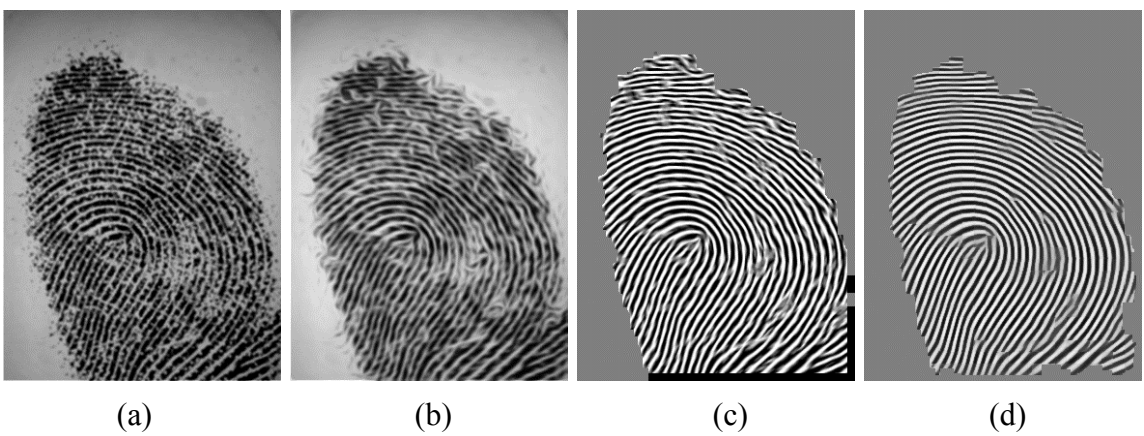
Figure 3.19 (a) Original image (FVC2004 (DB4A)), enhanced images after (b) first-stage, (c) second-stage and (d) third-stage.

In the second experiment, an original fingerprint image is enhanced by using the proposed method and the methods in [15] and [8]. The enhanced image by the proposed scheme is compared visually with that obtained using other two methods. Figure 3.20 (a) shows an original image and Figures (b), (c) and (d) the enhanced images by using the methods of [15], and [8] and the proposed scheme. It is seen from Fig 3.20 (b) that the method in [15] connects broken ridges. Since this method is quite sensitive to segmentation, it removes some ridges at the border of fingerprint image. It is seen from Fig 3.20(c) that the broken ridges are joined by the method in [8]; however, the ridges are not clearly visible due to poor contrast in the enhanced image near boundaries. The proposed method is seen to provide the best results in terms of the completeness of the ridges with improved contrast throughout the fingerprint image, as seen from the image in Fig 3.20 (d).

| (a) | (b) | (c) | (d) |
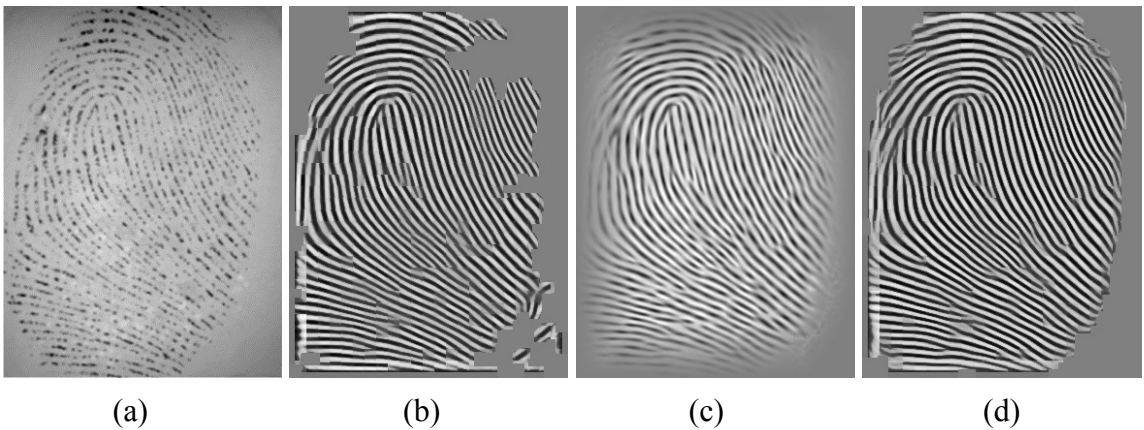
Figure 3.20 (a) Original image, (b) Enhanced image using method in [15], (c) Enhanced image using method in [8] and (d) Enhanced image using the proposed method.

In the third experiment, the subjective quality of the enhanced image is measured by a quality estimation method [41]. First, the orientation tensor Z of the fingerprint

image is computed and symmetry filters, h_n are designed using symmetry features of order n. The total symmetry image s is the summation of all the symmetry filter responses. For fingerprint image quality estimation, two symmetry filters are designed, namely linear and parabolic symmetry filter, depending on the value of n. In the former, the value of n is 0, whereas in the latter, it is ±1. The linear symmetry filter is to model typical ridge-valley flow, whereas the parabolic one is to define the flow around the singular regions. The values of n=1 and -1 indicate a core point and delta point, respectively.

The results of applying quality estimation method mentioned above are shown in Figure 3.21. The first row images in this figure are the original fingerprint image and those enhanced by methods in [15], and [8] and the proposed method. The second row of the figure shows the relevant total symmetry (summed magnitudes) $|s|$. The bright areas in $|s|$ indicate well-defined ridge-valley structure in both low (typical ridge-valley flow) and high curvature (singular points) region, whereas the dark areas indicate a low-quality structure.

Since the original image as seen in Figure 3.21(a) consisting of broken ridges, the symmetry in Figures 3.21 (e) shows a large amount of darker regions indicating poor quality. After applying the enhancement method in [15], the quality is improved as indicated by the bright regions in Figure 3.21 (f). However, some ridges missing near the boundaries of enhanced image in Figure 3.21 (f) produce dark regions at the corresponding areas Figure 3.21 (f). There are also some black areas inside the symmetry of Figure 3.21 (f), which indicates low quality ridge-valley structure in those regions. Although, the symmetry of image enhanced by the method in [8] consists of more bright

regions than the original, as illustrated by Figure 3.21 (g), there exist dark regions due to the low contrast near the boundaries of enhanced fingerprint image shown in Figure 3.21 (c). There are more black areas inside the symmetry of Figure 3.21 (g) more than in Figure 3.21(f), which indicates that the method of [15] is better than that of [8]. The proposed method is seen to provide the best result in terms of quality, as indicated by the bright and less dark areas of Figure 3.21 (h). It produces bright areas near boundaries as well as inside the symmetry, indicating well-defined ridge-valley structure in both normal and high curvature regions.

From the three experiments conducted in this section, it is seen that the proposed enhancement scheme is efficient in enhancing fingerprint images from different datasets.

| (a) | (b) | (c) | (d) |

| (e) | (f) | (g) | (h) |
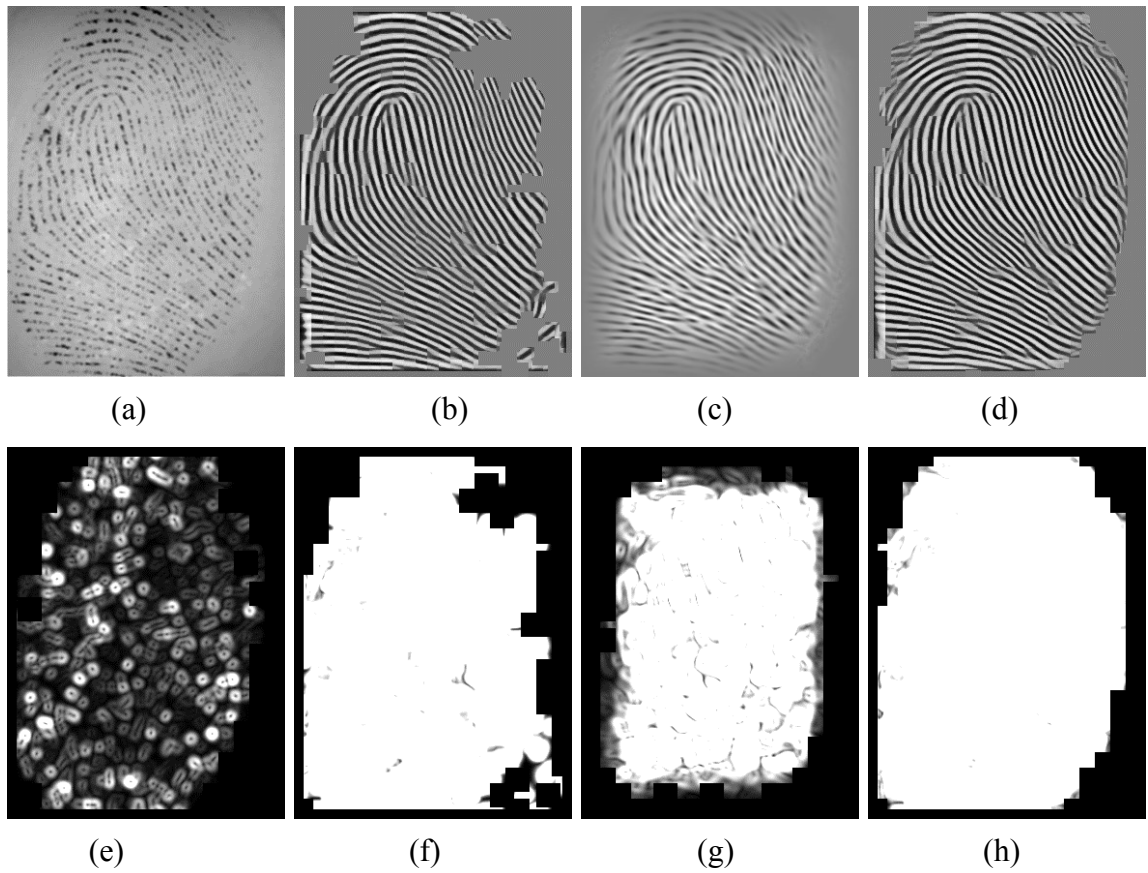
Figure 3.21 (a) An original image. Enhanced images by the (b) method in [15], (c) method in [8] and (d) proposed method. (e) - (h) Total symmetry (summed magnitudes) containing relevant portions $|s|$, corresponding to the images in (b), (c) and (d).

3.6.2 Objective Analysis

For the purpose of objective measurement of the performance of the proposed scheme, we perform two experiments: one in regard to quality of the enhanced image and the other in terms of complexity. In the first experiment, the qualities of the original and enhanced images by using the method in [15], and [8] and by the proposed method is measured using the quality estimation scheme described in the previous section. In the second experiment, the complexity of methods in [15], and [8] and the proposed method is measured in terms of the execution time of the enhancement schemes.

For the first experiment, the total symmetry image s, computed in the section 3.6.1, is divided into blocks. Then, the average of total symmetry image, $\bar{s}$ is computed. The correlation coefficient, $\bar{r}_{k,l}$ is obtained between any two orders. Then, the quantity $\bar{r}$ is computed as an average of the correlation coefficients. Next, the quality measure $\bar{q}$ for each block is computed by multiplying $\bar{s}$ with a monotonically decreasing function of $\bar{r}$. Finally, the quality of whole fingerprint image q is obtained by combining all the block quality measures. The values of the quality q are in the range $[0, q_{max}]$, where q_{max} >1. In this scale, a 0 represents the poorest quality, whereas unity indicating a normal quality and q_{max} represents the higher quality.

For the quantitative evaluation of the performance, the quality estimation method described above is applied on different databases. For each database, the average quality q and listed in Table 3.1. The table shows the average quality for the original and that of the enhanced images obtained by using the methods in [15], and [8] and the one proposed in this chapter. By comparing the results in this table, the following two observations can

be made. First, the quality of the original fingerprint images is improved significantly by using the proposed method. Second, the quality of enhanced images obtained by using the proposed method is better than that of the images obtained by using two recent schemes in [15] and [8]. Therefore, the proposed enhancement method is quite efficient in improving the quality of the fingerprint images both visually and quantitatively.

For the second experiment, the computation time is measured to evaluate the complexity performance of the proposed method. The proposed enhancement method with the three-stage filtering is implemented in MATLAB 2010 and the computation time is obtained based on the elapsed time. All the simulations are performed in the environment of Windows PC platform with a 2.40 GHz Duel Core AMD Opteron CPU and 3.37 GB RAM. The results are presented in Table 3.2. For the purpose of comparison, the table also gives the computation time using the methods [15] and [8]. It is seen from the results provided in this table demonstrate that the proposed method on an average takes 46% and 21% less time than the methods of [15] and [8], respectively. Thus, the proposed method provides an enhancement performance superior to that of [15] and [8] with a reduced computational cost.

Table 3.1 Average quality using different databases

Database	Original	Method [15]	Method [8]	Proposed Method
FVC2000	1.36	4.73	2.76	5.63
FVC2002	1.94	4.79	2.58	5.91
FVC2004	2.19	3.95	2.59	5.71

Table 3.2 Average processing times (in seconds) required by the methods [15], [8] and the proposed method using different databases.

		Method [15]	Method [8]	Proposed Method
FVC2000	DB1	14.3	12.3	8.7
	DB2	14.8	10.8	8.6
	DB3	35.4	23.9	20.2
	DB4	12.2	9.8	7.3
Average		19.2	14.2	11.2
FVC2002	DB1	23.3	17.3	13.6
	DB2	26.6	17.7	15.5
	DB3	14.2	12.2	8.5
	DB4	17.7	12.7	10.3
Average		20.5	14.9	11.9
FVC2004	DB1	49.8	28.4	24.9
	DB2	19.1	11.7	9.5
	DB3	23.2	14.6	11.1
	DB4	17.5	10.4	8.1
Average		27.4	16.3	13.4

3.7 Summary

In this chapter, a novel technique to enhance low-quality fingerprint image has been presented. The idea of combining the linear anisotropic diffusion filter, compensation filter and angular filter has been shown to be a promising methodology to improve the quality of fingerprint images. In this chapter, a comparative study of the iterative diffusion filter for enhancing a fingerprint image has been first undertaken in order to propose a simple and computationally efficient first-stage enhancement. It has been shown from this study that a simple estimation of the orientation field and small number of iterations can result in lowering the computational complexity of the first stage enhancement. The second stage filtering is carried out through a non-iterative ridge

compensation filtering, which overcomes the limitations of the first stage. The problem of blocking effect and limitations of the second stage filter has been solved with a third-stage filtering process. Unlike some other STFT approaches based on raised cosine spectral window for enhancing fingerprint images, in the proposed method, a Gaussian spectral window that reduces the blocking effect has been proposed. In order to show the effectiveness of the proposed method, the new scheme has been applied to a number of different databases with poor quality fingerprint images and the results have been compared with those obtained by using other existing methods. The subjective and objective results have clearly demonstrated the superiority of the proposed scheme in providing better-quality enhanced fingerprint images with a reduced computational cost.

Chapter 4

Effectiveness of the Proposed Enhancement Scheme in Fingerprint Recognition

4.1 Introduction

In the previous chapter, a three-stage filtering scheme to enhance fingerprint images has been proposed. In this chapter, the effectiveness and usefulness of the proposed enhancement scheme are examined in fingerprint feature extraction and matching for fingerprint recognition application. In Section 4.2, a minutiae extraction algorithm similar to the method in [42] is applied to the original and enhanced images in order to show the effectiveness of the proposed enhancement scheme. Next, in Section 4.3, a minutia-based matching algorithm is applied to the set of extracted minutiae using a hybrid shape and orientation descriptor in order to find similarity between two fingerprints. Finally in Section 4.4, extensive experiments on minutiae extraction and matching by applying them to original fingerprint images chosen from some challenging benchmark databases and on their proposed and other state-of-the-art enhancement schemes are conducted.

4.2 Minutiae Extraction

The reliability of minutiae-based fingerprint recognition systems depends on an accurate detection of fingerprint minutiae. Accurate extraction of minutiae is heavily dependent on the quality of the fingerprint image. Minutiae extraction methods are

mainly classified into two categories: 1) features extracted from the binary images of gray-scale fingerprints and 2) features extracted directly from gray-scale images.

In this section, minutiae are extracted in a way similar to that in the method of [42], that uses binary fingerprint image for feature extraction. This method consists of two steps: binarization and thinning. First, the gray-scale fingerprint image is transformed into a binary intensity of black (0) or white (1). This conversion is performed by applying a threshold value, *t,* to the image. The pixel values of the gray-scale image are compared with *t* to obtain a binary image. Any pixel value larger than the threshold is set to one and any value smaller than the threshold is set to zero, according to the equation:

$$I_b(x,y) = \begin{cases} 1, & if \ I(x,y) \geq t \\ 0, & otherwise \end{cases} \tag{4.1}$$

where *I(x,y)* is the grey-level fingerprint image and *t* is the global threshold. In second step, the binarized image *$I_b(x,y)$* undergoes a thinning operation which reduces the thickness of all ridges to a single pixel. The image obtained after the thinning operation, namely, the skeleton image contains the locations and orientations of the minutiae similar to that in the input fingerprint image. The skeleton/thinned image is obtained by applying a simple morphological thinning operation.

Next, the thinned binary image is analyzed in order to extract and store minutiae information. In order to obtain the minutiae information, the Rutovitz crossing number [1] is used within a 3×3 window centered at each pixel *p* as

$$cn(p) = \frac{1}{2}\sum_{i=1}^{8}\left|val(p_{(i\bmod 8)}) - val(p_{i-1})\right| \tag{4.2}$$

where *cn(p)* is the crossing number of a pixel *p* and *val(p)*∈{0,1} is the binary image pixel value. The crossing number is used to identify minutiae pixel location, as ridge ending having *cn=1*, bifurcation having *cn=3*, core point having *cn=5* and delta point having *cn>5* within the thinned image.

In order to show the effectiveness of the enhancement scheme proposed in the previous chapter, the above mentioned minutiae extraction algorithm is applied to: the original image and the enhanced image obtained using the scheme proposed in Chapter 3. The results are illustrated in the images of Figure 4.1 showing the extracted minutiae. We perform two analyses: subjective and objective. From a subjective point of view, it is seen that there are many false minutiae when the input is an original image as shown in Figure 4.1 (a). The proposed enhanced image in Figure 4.1(b) as an input contains smaller false minutiae than that the original image of Figure 4.1(a) does. Outside the fingerprint region, there are several false minutiae in the original image, whereas no false minutiae are present outside the fingerprint regions of the enhanced image. Also, the broken ridges in the original image are considered to generate false minutiae, whereas there are no such spurious minutiae in the enhanced image since broken ridges are completely joined.

From Figure 4.2 (a) it can be observed that the core point region is covered by smears in the original image. As a result, the core point (marked by green) detected incorrectly by the minutiae extraction method. The proposed enhancement scheme successfully removes smears from the original image which helps to detect the core point location correctly as shown in (b).
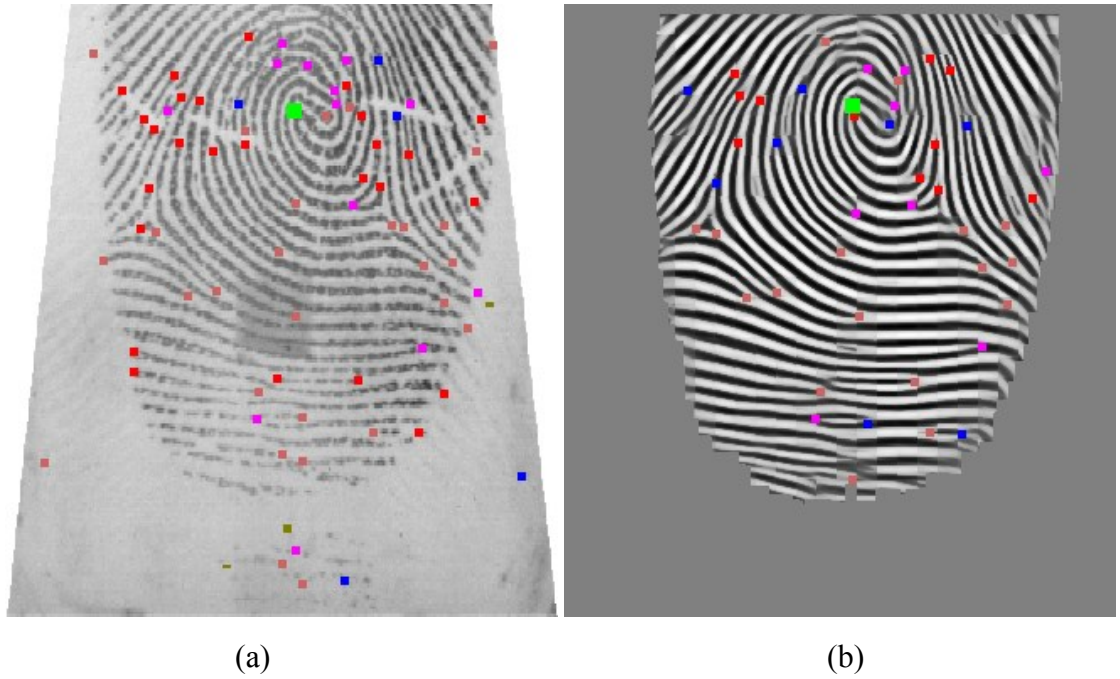
<center>(a)   (b)</center>

Figure 4.1 Minutiae from two input fingerprint images. (a) Original image. (b) Enhanced image obtained by the proposed method.

<center>(a)   (b)</center>
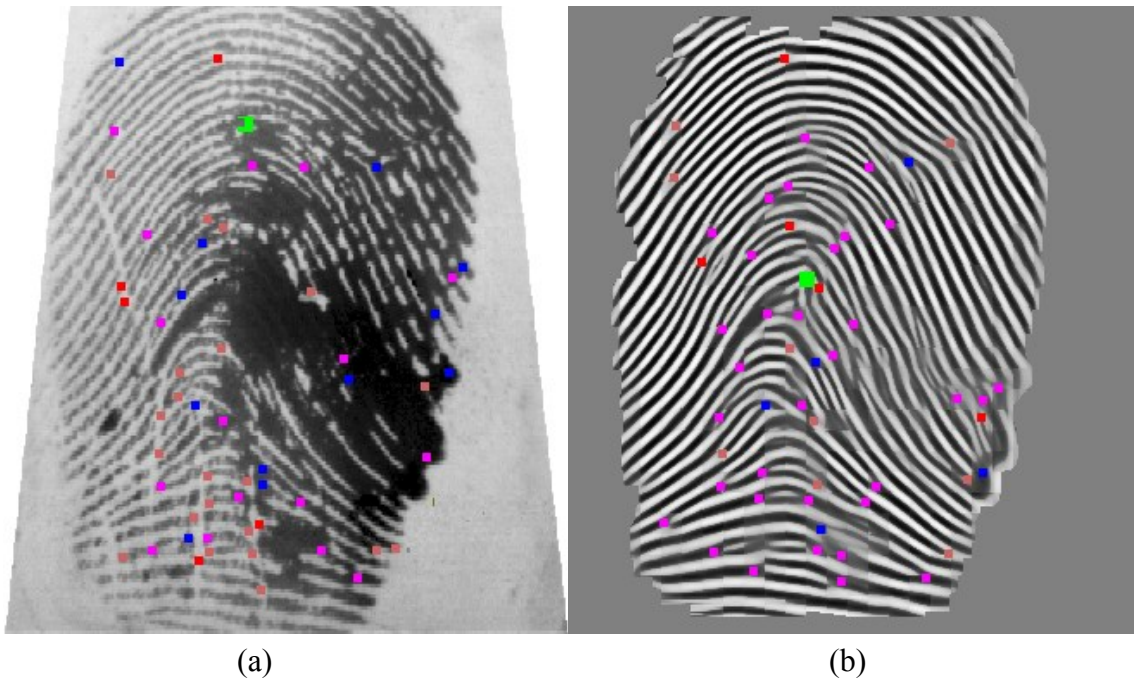
Figure 4.2 Minutiae core points (marked green) in two fingerprint images. (a) An original image from FVC2004 (DB2A). (b) Enhanced image by using the proposed method.

Figure 4.3 shows the extracted minutiae from the original image and from the enhanced images obtained by using the methods in [15], and [10] as well as by using the proposed enhancement method. By comparing Figures 4.3 (a) and (d), we can see that there are some missing minutiae (marked as circles) in the original image that these are successfully detected in the enhanced image. Figure 4.3 (b) shows the extracted minutiae from the enhanced image obtained by the method in [15]. It is seen that there are some missing ridge structure at the boundary of the fingerprint and the minutiae at these regions cannot be detected. From Figure 4.3 (c) which shows the enhaced image obtained by the method in [10] with its minutiae, it is seen that it consists of some spurious minutiae outside the fingerprint due to the artifacts produced by the method. The proposed method is seen to provide the best result in terms of minutiae extraction, as illustrated in Figure 4.3(d). It has less spurious and missed minutiae than the original fingerprint image or fingerprint images enhanced by the other methods do have.

| (a) | (b) | (c) | (d) |

Figure 4.3 Minutiae in four fingerprint images. (a) An original image. Enhanced images obtained by using (b) the method of [15], (c) the method of [10], and (d) the proposed method.
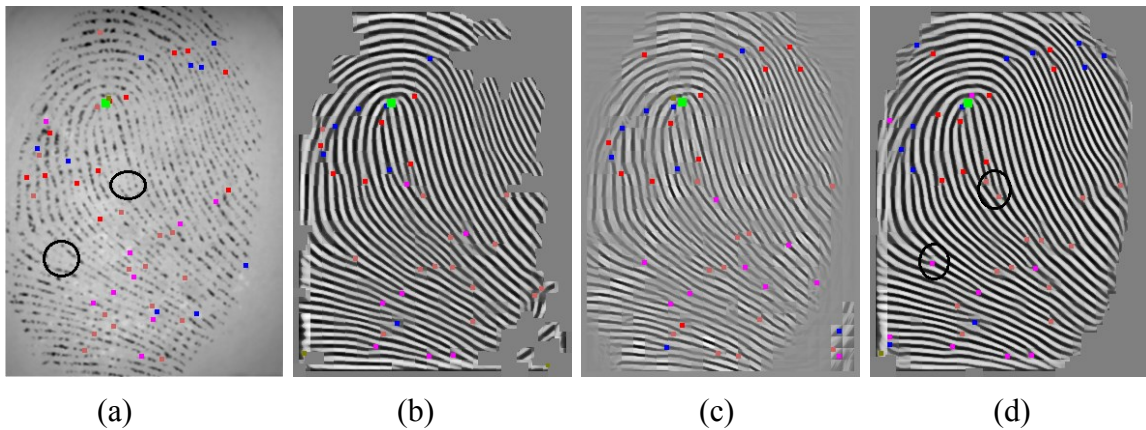
For an objective evaluation of minutiae extraction, the minutiae errors are computed using the original and images enhanced by methods in [15] and [10] as well as by the proposed method. We define the true minutiae ratio (TMR), false minutiae ratio (FMR), dropped minutiae ratio (DMR) and exchanged minutiae ratio (EMR) as the ratio of the number of true minutiae, false minutiae, dropped minutiae and exchanged minutiae to the number of total minutiae, respectively [43]. The true minutiae are the real minutiae within a fingerprint image. False minutiae are those that do not coincide with the true minutiae. Dropped minutiae are the real minutiae being missed during extraction process. Exchanged minutiae correspond to true minutiae with their types exchanged. Table 4.1, gives the results of average minutiae ratios and the total error in percentage using ten fingerprint images from the FVC2004 database. It is seen from this table that all the performance indices for minutiae extraction for images obtained by using the proposed enhancement scheme are superior to those for the original fingerprint images or to those for enhanced images obtained by other methods.

Table 4.1 Average TMR, FMR, DMR and EMR for original images and in their enhanced versions obtained by using the methods of [15] and [10] and the proposed method.

	Original Image	Method [15]	Method [10]	Proposed Method
TMR (%)	54.2	89.7	84.6	93.2
FMR (%)	27.4	3.5	5.4	2.9
DMR (%)	9.5	3.8	4.3	2.0
EMR (%)	8.9	3.0	5.7	1.9
Total Error = FMR+DMR+EMR (%)	45.8	10.3	15.4	6.8

4.3 Fingerprint Matching

In fingerprint matching, two fingerprint templates are compared based on the degree of similarity between the two fingerprint images. The matching decision of the two fingerprint images is based on a threshold. The value of the similarity score between 0 and 1 indicates whether or not the fingerprint under consideration is the same as the reference fingerprint. Matching schemes are concerned with: the accuracy of the final decision and the response time. However, the requirements of these two performance metrics vary from one application to another. Fingerprint matching algorithms can be classified into three different catergories: correlation-based, minutiae-based and non-minutiae based matching. Correlation-based matching superimposes two fingerprint images and computes the correlation between the corresponding pixels for different displacement and rotations. Minutiae-based matching extracts minutiae from two fingerprints and stores them as sets in order to find maximum number of pairings from the alignment between the sets. Non-minutiae based matching uses more reliable features (e.g. ridge shape, orientation, frequency) rather than minutiae in order to align and match two fingerprint images.

In this section, a matching algorithm proposed by Abraham et al. [42] based on a hybrid shape and orientation descriptor is applied to both the original and enhanced images. This method consists of two steps: adaptive greedy registration and matching.

4.3.1 Adaptive Greedy Registration

In minutiae-based matching algorithm, a minutia, m_i, is described as $m_i = \{x, y, \theta\}$ where (x, y) indicates the location and θ is the orientation of the minutia. The minutiae set of a test image A is

$$A = \{m_{A_1}, m_{A_2}, \ldots\ldots, m_{A_p}\} \tag{4.3}$$

where $m_{A_i} = \{x_{A_i}, y_{A_i}, \theta_{A_i}\}$, $\{x_{A_i}, y_{A_i}\}$ is the location of ith minutia of the test image A and θ_{A_i} is the corresponding orientation.

The minutiae set of a template image B is

$$B = \{m_{B_1}, m_{B_2}, \ldots\ldots, m_{B_q}\} \tag{4.4}$$

where $m_{B_j} = \{x_{B_j}, y_{B_j}, \theta_{B_j}\}$, $\{x_{Bj}, y_{Bj}\}$ is the location of jth minutia of the test image B and θ_{B_j} is the corresponding orientation. The minutiae-based matching performs pairing of minutiae points from the test image A minutiae set to that of the template image B.

Using (4.3) and (4.4), minutiae pairs are formed based on the geometric distance and the orientation difference computed as

$$dist_r\left(m_{A_i}, m_{B_j}\right) = \sqrt{\left(x_{A_i} - x_{B_j}\right)^2 + \left(y_{A_i} - k_y \cdot y_{B_j}\right)^2} \tag{4.5}$$

where

$$\sqrt{\left(x_{A_i} - x_{B_j}\right)^2 + \left(y_{A_i} - y_{B_j}\right)^2} < r_\delta$$

and

$$dist_\theta\left(m_{A_i}, m_{B_j}\right) = \min\left(\left|\theta_{A_i} - \theta_{B_j}\right|, 360^0 - \left|\theta_{A_i} - \theta_{B_j}\right|\right) \qquad (4.6)$$

where

$$\min\left(\left|\theta_{A_i} - \theta_{B_j}\right|, 360^0 - \left|\theta_{A_i} - \theta_{B_j}\right|\right) < r_\theta$$

In the above r_δ and r_θ are the tolerance for the distortion and angular differences, k_y is an empirically chosen parameter. A metric of similarity, called the similarity score, is computed using minutiae pairs as

$$S\left(m_{A_i}, m_{B_j}\right) = \left(\frac{1}{K}\right) \sum_c^L \sum_d^{K_c} \exp\left(\frac{2\left(\min\left|\theta_{c,d}^{A_i} - \theta_{c,d}^{B_j}\right|, \pi - \left|\theta_{c,d}^{A_i} - \theta_{c,d}^{B_j}\right|\right)}{\pi\mu}\right) \qquad (4.7)$$

where $S\left(m_{A_i}, m_{B_j}\right) < \delta_S$, the orientation descriptor has a total of K sample points distributed as L concentric circles having K_c points (i.e., possibly differing number per circle) with equidistant angular distribution (i.e. the step of size $\frac{2\pi}{K_c}$), $\theta_{c,d}^{A_i}$ is minimum angle required to rotate the dth sample orientation on the cth circle to the orientation of the minutia m_{A_i} (likewise for $\theta_{c,d}^{B_j}$), and μ and δ_S are empirically chosen parameters. The cost of matching is computed in two steps: affine and non-affine components.

First, the cost of matching two minutiae for affine components is computed as

$$C^{**}\left(p_i, q_j\right) = \left(\frac{1}{2} \sum_{k=1}^{K} \frac{\left[h_{p_i}(k) - h_{q_j}(k)\right]^2}{\left[h_{p_i}(k) + h_{q_j}(k)\right]^2} \times \exp\left(-\frac{r_k - r_{min}}{2\sigma^2}\right)\right) \qquad (4.8)$$

where P and Q are the minutiae sets of fingerprints A and B, respectively, h_{p_i} and h_{q_j} denote the K-bin histograms of points p_i and q_j, respectively, r_k is the current bin outer boundary distance, $r_{\min}$ is the outer boundary of the closest bin, σ^2 is a tunable parameter. Now, the shape similarity distance for the affine components is computed using

$$D_{SC}(P,Q) = \frac{1}{n}\sum_{p_i \in P} \arg \min_{q_j \in Q} C^{**}(p_i, q_j) + \frac{1}{m}\sum_{q_j \in Q} \arg \min_{p_i \in P} C^{**}(p_i, q_j) \qquad (4.9)$$

where $D_{SC}(P,Q) < \delta_{SC}$, n and m are minutiae from test and template fingerprints, P and Q, respectively, and δ_{SC} is an empirically chosen parameter. Now, the nearest neighbor set Φ_α is evaluated by

$$\Phi_\alpha = \{i \mid \sqrt{\left(x_{A_i} - x_{B_j}\right)^2 + \left(y_{A_i} - y_{B_j}\right)^2}\} \qquad (4.10)$$

where $\{i \mid \sqrt{\left(x_{A_i} - x_{B_j}\right)^2 + \left(y_{A_i} - y_{B_j}\right)^2}\} < \delta_N$, Φ_α consisting of all interior nearest neighbor indices from fingerprint A, and likewise, Φ_β consisting of all interior nearest neighbor indices from fingerprint B. The corresponding anchor point set Φ_ψ is computed as

$$\Phi_\psi \subseteq \{(i,j) \mid i \in \Phi_\alpha \text{ and } j \in \Phi_\beta\} \qquad (4.11)$$

Secondly, the cost of matching two minutiae for non-affine components is computed as

$$C^\gamma(p_i, q_j) = \gamma_d \gamma_\theta C^{**}(p_i, q_j) \qquad (4.12)$$

where γ_d and γ_θ are defined as

$$\gamma_d = \begin{cases} 1 & \text{if } dist(p_i, q_j) < \delta_{\max} \\ \infty & \text{otherwise} \end{cases} \qquad (4.13)$$

and

$$\gamma_\theta = \begin{cases} 1, & \text{if } \min\left(\left|\theta_{A_i} - \theta_{B_j}\right|, \pi - \left|\theta_{A_i} - \theta_{B_j}\right|\right) < \theta_{\max} \\ \infty, & \text{otherwise} \end{cases} \qquad (4.14)$$

$\delta_{\max}$ and $\theta_{\max}$ being the maximum feasible distance and orientation caused by warping after applying the candidate affine transform and orientation estimation error in the extraction process, respectively. The shape similarity distance for non-affine components D_{be} is computed using a method similar to that in [44].

Finally, the total shape similarity distance/ shape context can be measured as

$$D_{SC}^{**}(P, Q) = \frac{1}{n_R} \sum_{p_i \in P \mid S\left(m_{A_i}, m_{B_j}\right) < \delta} \left(C^\gamma(p_i, q_j) + \Lambda.S\left(m_{A_i}, m_{B_j}\right)\right) + \beta D_{be} \qquad (4.15)$$

where $S\left(m_{A_i}, m_{B_j}\right)$ is scaled by a tunable parameter Λ with range [0,1] and n_R is the number of iterations.

4.3.2 Matching Based on Hybrid Shape and Orientation Descriptor

Once the minutiae pairs have been established, a similarity score is computed to describe as to how similar the two fingerprints are, taking into account all of the relevant information obtained from the previous section, such as the number of genuine minutiae

pairs and how similar each pair is. The fingerprint matching similarity score is computed as

$$sim(A,B) = \frac{n_M \left(\sum_{(i,j)} sim_\delta \left(m_{A_i}, m_{B_j} \right) \right) \cdot \left(\sqrt{S_{\max}} \right)}{n_A n_B} - vD_{SC}^{**} \tag{4.16}$$

where $S_{\max} = \arg\max_{(i,j)} S^* \left(m_{A_i}, m_{B_j}, I(A_i, B_j) \right)$, n_M is the number of matching filtered minutiae pairs, n_A and n_B are the number of minutiae in the overlapped region from the fingerprints A and B, respectively, i and j are the indices of the filtered minutiae pair elements in the fingerprints A and B, respectively and v a tunable parameter in the range $[0,1]$.

The orientation-based descriptor similarity measure relies on the intersection set $I_{SC}(A_i, B_j)$ indicating as to which samples only are to be used for the similarity calculation and this set is defined as

$$I_{SC}(A_i, B_j) = \left\{ s \mid s \in \{L, K_c\} \text{ and valid } \left(A(s_x, s_y) \right) \right\} \cap \left\{ t \mid t \in \{L, K_c\} \text{ and valid } \left(B(t_x, t_y) \right) \right\} \tag{4.17}$$

where L is the sample position set and K_c is the concentric circle set. The similarity measure defined as

$$S^* \left(m_{A_i}, m_{B_j}, I \right) = S \left(m_{A_i}, m_{B_j} \right) \times \exp \left(-\max \left(0, \Delta_{cutoff - \Delta_{g\_count}} \right) \cdot \mu_s \right) \tag{4.18}$$

where Δ_{cutoff} is the cutoff point such that all the good sample totals below this value are weighed, Δ_{g_count} is the total number of good samples, and μ_s is a tunable parameter,

A δ-neighbourhood similarity score is tallied for the candidate minutiae pair $\left(m_{A_i}, m_{B_j}\right)$ for each matched δ-neighbourhood minutiae pair having respective neighbourhood sorted set indices (x_s, y_t), also found to match, using

$$sim_\delta\left(m_{A_i}, m_{B_j}\right) = \sum_{s,t}\left(\alpha(x_s, y_t) + \gamma\beta(x_s, y_t)\right) \tag{4.19}$$

where

$$\alpha(x, y) = \exp\left(-r_{diff\left(m_{A_i}, m_{B_j}\right)}(x, y) - \theta_{diff\left(m_{A_i}, m_{B_j}\right)}(x, y) - \angle_{diff\left(m_{A_i}, m_{B_j}\right)}(x, y)\right) \tag{4.20}$$

and

$$\beta(x, y) = \exp\left(-\Gamma_{diff\left(m_{A_i}, m_{B_j}\right)}(x, y)\right) \tag{4.21}$$

with a tunable parameter γ defined in [0,1]

The distance $r_{diff\left(m_{A_i}, m_{B_j}\right)}(x, y)$, orientation $\theta_{diff\left(m_{A_i}, m_{B_j}\right)}(x, y)$, and angle $\angle_{diff\left(m_{A_i}, m_{B_j}\right)}(x, y)$ are computed as

$$r_{diff\left(m_{A_i}, m_{B_j}\right)}(x, y) = \left|d_{A_{i(x)}} - d_{B_{j(y)}}\right|, \tag{4.22}$$

$$\theta_{diff\left(m_{A_i}, m_{B_j}\right)}(x, y) = \min\left(\left|\theta_{A_{i(x)}} - \theta_{B_{j(y)}}\right|, \pi - \left|\theta_{A_{i(x)}} - \theta_{B_{j(y)}}\right|\right), \tag{4.23}$$

$$\angle_{diff\left(m_{A_i}, m_{B_j}\right)}(x, y) = \min\left(\left|\angle_{A_{i(x)}} - \angle_{B_{j(y)}}\right|, 2\pi - \left|\angle_{A_{i(x)}} - \angle_{B_{j(y)}}\right|\right) \tag{4.24}$$

The texture $\Gamma_{diff\left(m_{A_i}, m_{B_j}\right)}(x, y)$ is composed of the set of all orientation samples and is used to dynamically calculate the orientation difference of neighbouring minutiae for a minutiae pair's respective δ-neighbourhoods, using

$$\Gamma_{diff\left(m_{A_i}, m_{B_j}\right)}(x, y) = \left|\Gamma_{A_{i(x)}} - \Gamma_{B_{j(y)}}\right| \tag{4.25}$$

where $\Gamma_{A_{i(x)}} = S^* \left(m_{A_i}, m_{A_{i(x)}}, I_0 \right)$, $\Gamma_{B_{j(y)}} = S^* \left(m_{B_j}, m_{B_{j(y)}}, I_0 \right)$ with the overlap index set given by $I_0 = I\left(A_i, A_i(x) \right) \cap I\left(B_j, B_j(y) \right)$

4.4 Performance Results and Comparison

In this section, experimental results on the effectiveness of fingerprint image enhancement on fingerprint recognition are presented. In order to do so, first, the recognition accuracy of the fingerprint matching technique described in the previous section, in terms of equal error rate (EER) and receiver operating characteristic (ROC) curves, is obtained by applying this matching technique on some original fingerprint images and their enhanced versions obtained by the scheme of [10] and one proposed in Chapter-3. Then, the average CPU time for fingerprint template formulation and for fingerprint matching using the same matching scheme are obtained for the original fingerprint images and for their two enhanced versions.

Table 4.2 gives the EER rate of the matching scheme described in the previous section with no fingerprint image enhancement, and the enhancement of the method of [10] and that of the proposed scheme using fingerprint images from the databases FVC2002 and FVC2004. It is seen from this table that the EER performance is better for the fingerprint images enhanced by using the three-stage scheme than that for the original image or the images enhanced by the method of [10].

Figures 4.4 depicts the ROC curves provided for fingerprint images with no enhancement and with the enhancement using the method of [10] and proposed method on database FVC2002 (DB1 and DB2). These ROC curves show that the overall recognition accuracy of the enhanced images obtained by the proposed enhancement

technique is much higher than that of the enhanced images obtained by using the method of [10] or the original images for both sub-databases.

Table 4.2 EER(%) using original and enhanced fingerprint images

Fingerprint Images	FVC2002		FVC2004	
	DB1	DB2	DB1	DB2
Original	9.36%	29.36%	31.43%	37.22%
Enhanced by method in [10]	2.17%	14.29%	28.09%	4.76%
Enhanced by proposed	1.42%	13.63%	18.57%	4.28%

It is also seen from the ROC curves of Figure 4.4 that the accuracy result with the fingerprint images obtained by the proposed enhancement scheme is slightly better than that with the images enhanced by the method of [10] is slightly inferior in the region of FMR < 0.2% for FVC2002 (DB1) fingerprint images and in the region of FMR > 10% for FVC2002 (DB2) fingerprint images.

Figures 4.5 depicts the ROC curves provided for fingerprint images with no enhancement and with the enhancement using the method of [10] and proposed method on database FVC2004 (DB1 and DB2). These ROC curves show that the overall recognition accuracy of the enhanced images obtained by the proposed enhancement technique is much higher than that of the enhanced images obtained by using the method of [10] or the original images for both sub-databases.
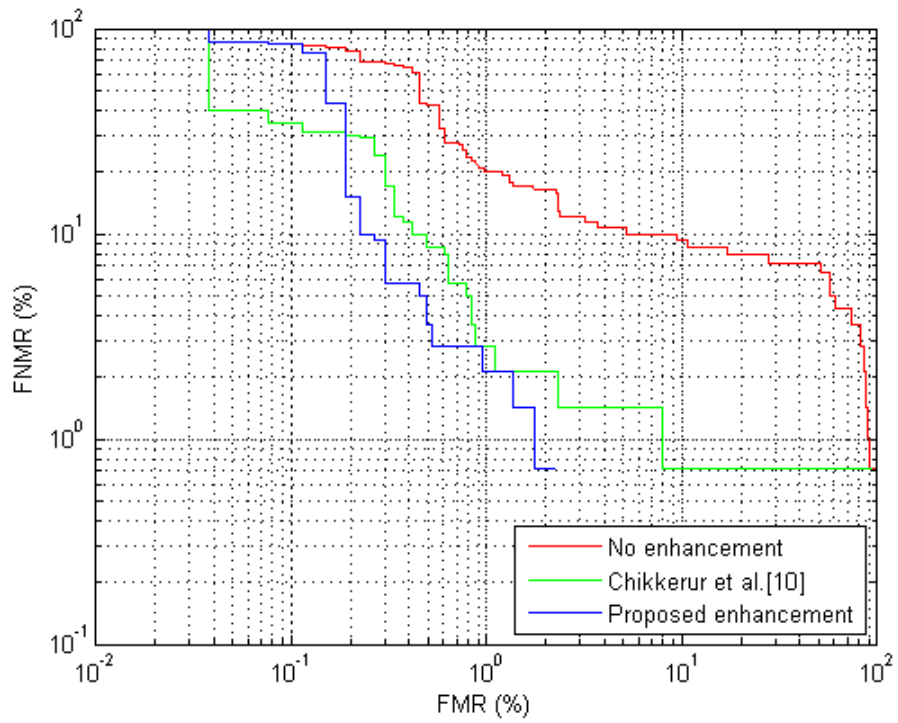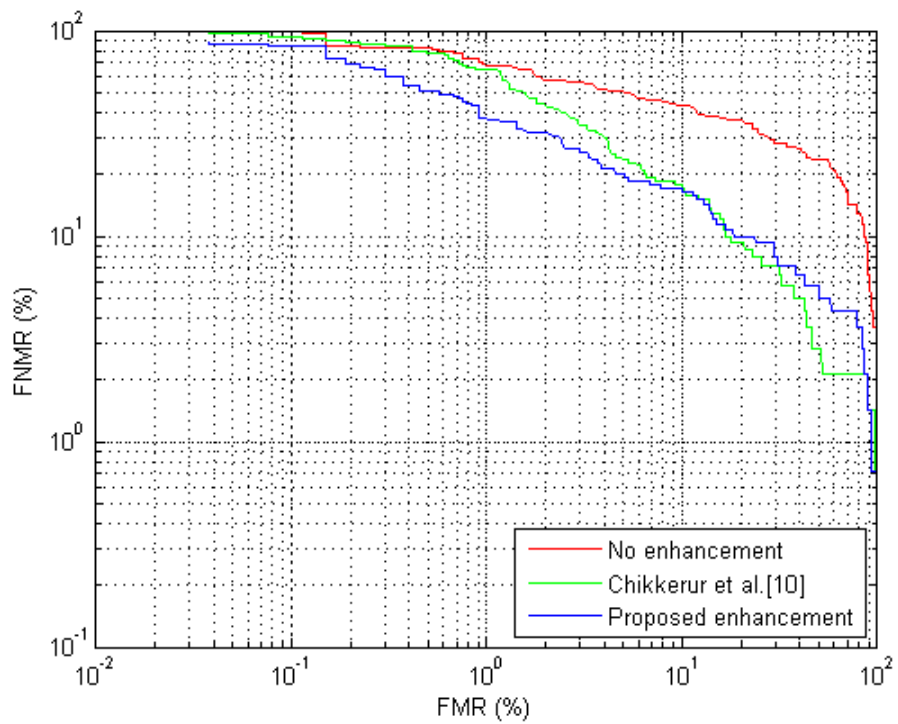
It is also seen from the ROC curves of Figure 4.5 that the accuracy result with the fingerprint images obtained by the proposed enhancement scheme is slightly better than that with the images enhanced by the method of [10] is slightly inferior in the region of
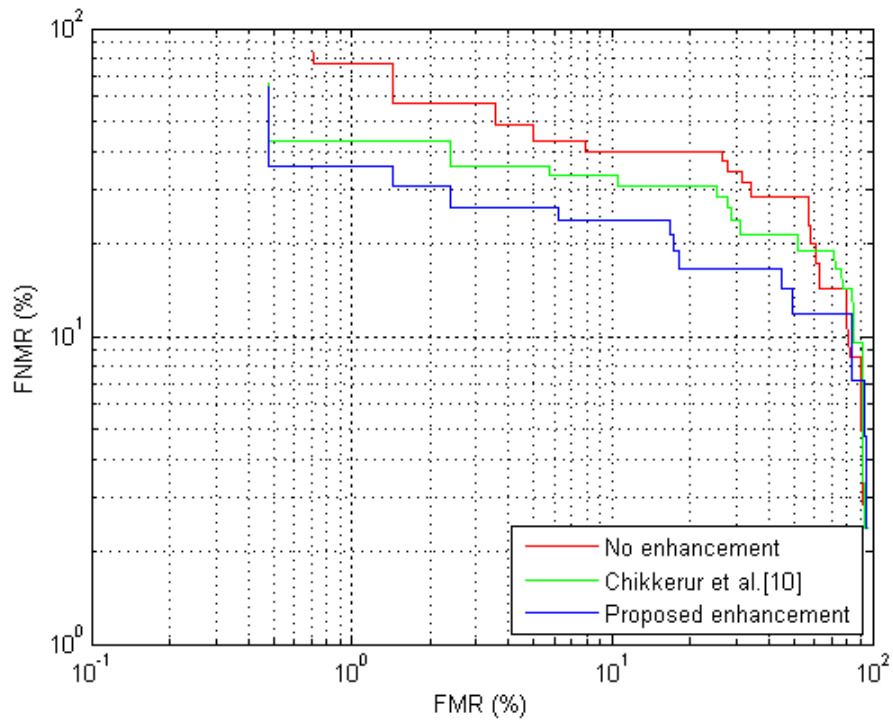
(a)

(b)

Figure 4.4 ROC curves for FVC2002 (a) DB1 and (b) DB2 fingerprint original and enhanced images obtained by using the scheme of [10] and the proposed scheme.
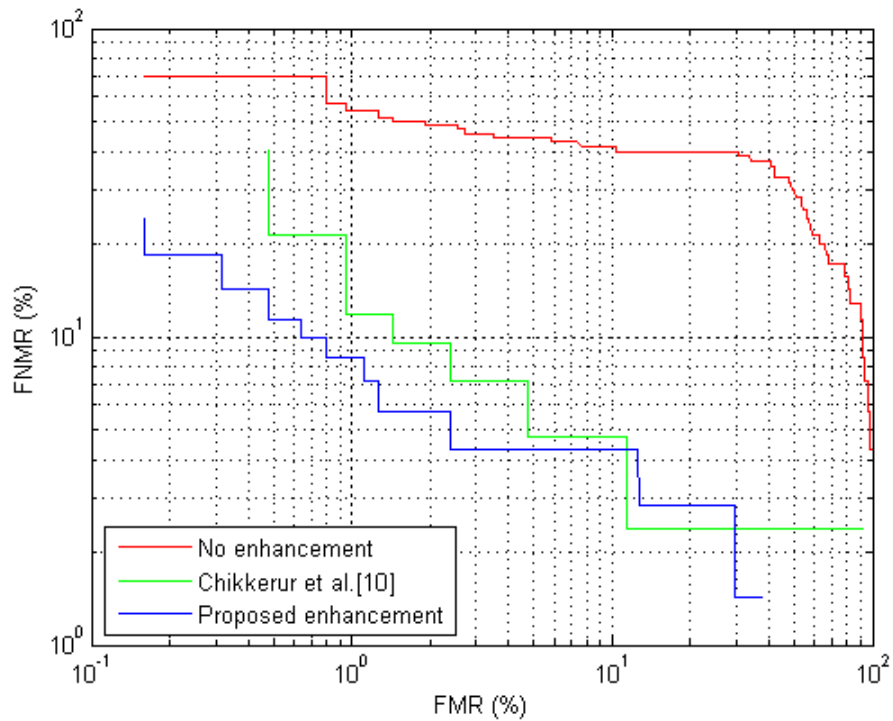
(a)

(b)

Figure 4.5 ROC curves for FVC2004 (a) DB1 and (b) DB2 fingerprint original and
enhanced images obtained by using the scheme of [10] and the proposed
scheme.

FMR > 80% for FVC2004 (DB1) fingerprint images and in the region of FMR > 10% for FVC2004 (DB2) fingerprint images.

Table 4.3 provides the CPU times of implementing the fingerprint template formulation and matching for fingerprint images with and without an enhancement. In this table, by comparing the CPU times required for the fingerprint template formulation and matching applied on fingerprint images enhanced by the proposed scheme, in general, less than that required by the original fingerprints and enhanced images obtained by using the method of [10].

Table 4.3 CPU times (s) for the fingerprint template formulation and matching scheme using the scheme of section 4.3 for original and enhanced fingerprint images using the scheme of [10] and the proposed scheme

Module	Fingerprint Image	FVC2002		FVC2004	
		DB1	DB2	DB1	DB2
Template formulation	With no enhancement	23.1	26.6	41.17	28.59
	Enhancement using method in [10]	25.6	32.2	44.63	22.09
	Enhancement using the proposed scheme	20.5	24	35.76	21.26
Matching	With no enhancement	8.2	5.1	32.5	68.9
	Enhancement using method in [10]	6.7	6.8	23.4	41.3
	Enhancement using the proposed scheme	3.9	4.6	21.3	16.4

4.5 Summary

Ability of a fingerprint recognition algorithm is very much dependant of the quality of the fingerprint image. In Chapter 3, a three-stage fingerprint enhancement technique was developed to improve the quality of fingerprint images by using one global

feature (namely, the orientation field). In this chapter, it has been first demonstrated that true minutiae extraction ratio can be significantly increased with the use of fingerprint images enhanced by using the scheme proposed in Chapter 3. Because of the increased minutiae extraction ratio using the proposed enhancement scheme, a minutiae-based fingerprint matching technique has then been described for fingerprint recognition.

In order to show the effectiveness of the proposed three-stage fingerprint image enhancement scheme, extensive experiments have been performed in fingerprint recognition by applying the minutiae-based matching technique on FVC2002 and FVC2004 databases. It has been shown that the proposed fingerprint image enhancement scheme has a significant impact on the recognition performance of the minutiae-based matching technique, in terms of its receiver operating characteristic, equal error rate, and CPU times of template formulation and fingerprint matching.

Chapter 5

Conclusion and Scope for Future Work

5.1 Concluding Remarks

Fingerprints are the best universal personal identifier amongst all biometrics. There are two major steps in the recognition systems using fingerprints: 1) accurate feature extraction of fingerprints, and 2) fingerprint matching using the extracted features in order to find the similarity between two fingerprints. These two steps heavily depend on the quality of the fingerprint image. Fingerprint enhancement is the most commonly used operation to improve the feature extraction and matching performances in a fingerprint recognition system. Presence of broken ridges, smears, scars/creases and falsely connected ridges in fingerprint image can make the task of enhancement a difficult problem. Many methods have been proposed to overcome these difficulties in order to improve the quality of fingerprint images. However, these schemes result in an increased complexity in enhancing fingerprint images, since these schemes rely on accurate computation of global features (e.g. ridge orientation, ridge frequency, etc.). The computational time is adversely affected due to the need for accurate estimation of global features. Further, most of the enhancement techniques use block image processing operation. As a result, the quality of the fingerprint image suffers from the blocking effect. This thesis has been concerned with the development of a computationally efficient technique for fingerprint enhancement, that can meet not only the challenges arising from the need for accurate estimation of global features of the fingerprints, but

also deal effectively with the problems resulting from the block processing of fingerprint images.

In the first part of the thesis, a low-complexity three-stage fingerprint enhancement scheme, using the fingerprint orientation field, has been developed. The main focus of the proposed scheme has been on overcoming the problems resulting from the need for accurate estimation of global features of fingerprint images. The problem of complex method for an accurate estimation of global features is solved by considering only one global feature, i.e., the orientation field, and computing it using a simple gradient-based method. For the purpose of computing the image gradients, Gaussian operator is used and the orientation field is determined by making used of these gradients. In the proposed enhancement technique, the orientation field has been obtained by using some simple mathematical operations. Another distinguishing characteristic of the proposed method is that, unlike some other enhancement schemes for fingerprint images in which larger number of iterations are required, a reduced number of iterations is utilized. The problem of blocking effect has been investigated by treating it as that of selecting a spectral window used in short time Fourier transform analysis. For the purpose of reducing the blocking effect, a Gaussian spectral window has been designed and used. The Gaussian spectral window puts more weight at the center and less weight at the edge. An attribute of the window leading to the computational simplicity of the proposed enhancement technique is in its ability to reduce blocking effect in the enhanced fingerprint image. The use of simple orientation field estimation, small number of iterations and Gaussian spectral window provides a computationally simple as well as efficient method for fingerprint image enhancement.

In the second part of the thesis, it has been demonstrated that true minutiae extraction rate can be significantly increased with the use of fingerprint images enhanced by using the proposed enhancement scheme. Because of the increased minutiae extraction rate resulting from the use of the proposed enhancement scheme, a minutiae-based fingerprint matching technique has then been described for fingerprint recognition.

In order to show the effectiveness of the proposed three-stage fingerprint image enhancement scheme in fingerprint recognition problems, extensive experiments have been performed by applying the minutiae-based matching technique on the FVC2002 and FVC2004 databases. It has been shown that the proposed fingerprint image enhancement scheme has a significant impact on the recognition performance of a minutiae-based matching technique, in terms of its receiver operating characteristic, equal error rate, and CPU times of template formulation and fingerprint matching.

5.2 Scope for Future Investigation

The research work undertaken in this thesis has focused on developing an efficient technique for enhancing low-quality fingerprint images with less computation time. Although the performance of the proposed method has been shown to be superior to that provided by three other techniques in the literature, there are a number of other studies that could be undertaken to further improve the quality of fingerprint images and reduce the computational complexity.

1. More global features (e.g., ridge frequency, singular points) and local features (e.g., minutiae) could be included to design the filters to further improve the quality of fingerprint images.

2. A study could be undertaken for developing fingerprint indexing technique using fingerprint images enhanced using the proposed scheme to reduce the matching time in fingerprint identification applications.

3. The proposed algorithm could be made faster by implementing it in C/C++.

4. Recently, researchers are investigating feature extraction and identification for very challenging fingerprint images such as latent fingerprints. Latent fingerprint image consists of a weak fingerprint buried in the midst of structured and noisy background. Pre-processing is required to effectively segment the fingerprint region from the background and also enhance the quality of broken ridge/valley patterns. The proposed method could be modified to be considered as a pre-processing stage to enhance the latent fingerprint images.

REFERENCES

[1] D. Maltoni, D. Maio, A.K. Jain and S. Prabhakar, "Handbook of Fingerprint Recognition," 2nd ed., Springer, 2009.

[2] L. Hong, Y. Wang and A. K. Jain, "Fingerprint image enhancement: Algorithm and performance evaluation," *IEEE Trans. Pattern Analysis and Machine Intelligence.*, vol. 20, no. 8, pp. 777–789, 1998.

[4] V. Areekul, U. Watchareeruetai, K. Suppasriwasuseth and S. Tantaratana, "Separable Gabor filter realization for fast fingerprint enhancement," *Proc. IEEE Int. Conf. Image Processing,* Genova, vol. 3, pp. 253-256, 2005.

[5] E. K. Yun and S. B. Cho, "Adaptive Fingerprint Image Enhancement with Fingerprint Image Quality Analysis," *Image and Vision Computing*, vol. 24, no. 1, pp. 101–110, 2006.

[6] R. Hastings, "Ridge enhancement in fingerprint images using oriented diffusion," *Proc. Ninth Conf. on Digital Image Computation Technology and Application*, Glenelg, Australia, pp. 245‑252, 2007.

[7] Q. Zhao, L. Zhang, D. Zhang, W. Huang and J. Bai, "Curvature and singularity driven diffusion for oriented pattern enhancement with singular points," *Proc. Conf. on Computer Vision and Pattern Recognition (CVPR)*, pp. 2129‑2135, Miami, FL, USA, 2009.

[8] C. Gottschlich and C.-B. Schönlieb, "Oriented diffusion filtering for enhancing low-quality fingerprint images," *IET biometrics,* vol. 1, no. 2, pp. 105-113, 2012.

[9] B.G. Sherlock, D.M. Monro and K. Millard, "Fingerprint Enhancement by Directional Fourier Filtering," *Vision, Image and Signal Processing,* vol. 141, no. 2, pp. 87-94, 1994.

[10] S. Chikkerur, A.N. Cartwright and V. Govindaraju, "Fingerprint enhancement using STFT analysis," *Pattern Recognition,* vol. 40, no. 1, pp. 198-211, 2007.

[11] S. Jirachaweng and V. Areekul, "Fingerprint enhancement based on discrete cosine transform," *Proc. International Conference on Advances in Biometrics,* pp. 96-105, 2007.

[12] C.T. Hsieh, E. Lai and Y.C. Wang, "An effective algorithm for fingerprint image enhancement based on wavelet transform," *Pattern Recognition,* vol. 36, no. 2, pp. 303-312, 2003.

[13] W. Zhang, Y. Tang and X. You, "Fingerprint enhancement using wavelet transform combined with Gabor filter," *Int. J. of Pattern Recognition and Artificial Intelligence,* vol. 18, no. 8, pp. 1391-1406, 2004.

[14] J. Lei, Q. Peng, X. You, H. H. Jabbar and P. S. P. Wang, " Fingerprint enhancement based on wavelet and anisotropic filtering," *Int. J. of Pattern Recognition and Artificial Intelligence,* vol. 26, no. 1, pp. 1256001-1-15, 2012.

[15] J. Yang, N. Xiong and A.V. Vasilakos, "Two-stage enhancement scheme for low-quality fingerprint images by learning form the images," *IEEE Trans. Human-Machine Systems,* vol. 43, no. 2, pp. 235-248, 2013.

[16] P. Sutthiwichaiporn and V. Areekul, "Adaptive boosted spectral filtering for progressive fingerprint enhancement," *Pattern Recognition,* vol. 46, no. 9, pp. 2465-2486, 2013.

[17] S. Jirachaweng, Z. Hou, J. Li, W.Y. Yau and V. Areekul, "Residual orientation modeling for fingerprint enhancement and singular point detection," *Pattern Recognition,* vol. 44, no. 2, pp. 431–442, 2011.

[18] S. Greenberg, M. Aladjem and D. Kogan, "Fingerprint image enhancement using filtering techniques," *Real-Time Imaging,* vol. 8, no. 3, pp. 227–236, 2002.

[19] C. Gottschlich, "Curved-region-based ridge frequency estimation and curved Gabor filters for fingerprint image enhancement," *IEEE Transactions on Image Processing,* vol. 21, no. 4, pp. 2220–2227, 2012.

[20] J. Yang, L. Liu, T. Jiang and Y. Fan, "A modified Gabor filter design method for fingerprint image enhancement," *Pattern Recognition Letters,* vol. 24, no. 12, pp. 1805–1817, 2003.

[21] R. Cappelli, D. Maltoni and F. Turroni, "Fingerprint Enhancement using Contextual Iterative Filtering," *Proc. of the 5th International Conference on Biometrics,* pp. 152–157, 2012.

[22] S. Ram, H. Bischof and J. Birchbauer, "Modeling fingerprint ridge orientation using Legendre polynomials," *Pattern Recognition,* vol. 43, no. 1, pp. 342–357, 2010.

[23] M. A. Oliveira and N.J. Leite, "A multiscale directional operator and morphological tools for reconnecting broken ridges in fingerprint images," *Pattern Recognition,* vol. 41, no. 1, pp. 367-377, 2008.

[24] S. Wang and Y. Wang, "Fingerprint enhancement in the singular point area," *IEEE Signal Processing Letters,* vol. 11, no. 1, pp. 16–19, 2004.

[25] W. Wang, J. Li, F. Huang and H. Feng, "Design and implementation of Log-Gabor filter in fingerprint image enhancement," *Pattern Recognition Letters,* vol. 29, no. 3, pp. 301–308, 2008.

[26] P. Sutthiwichaiporn, V. Areekul and S. Jirachaweng, "Iterative fingerprint enhancement with matched filtering and quality diffusion in spatial-frequency domain," *Proc. of International Conference on Pattern Recognition,* pp. 1257–1260, 2010.

[27] A.J. Willis and L. Myers, "A cost–-effective fingerprint recognition system for use with low-quality prints and damaged fingertips," *Pattern Recognition,* vol. 34, no. 2, pp. 255–270, 2001.

[28] S. Gaur, V. A. Shah and M. Thakker, "Biometric recognition technique: A review," *Int. J. Advanced Research in Electrical, Electronics and Instrumentation Engineering,* vol. 1, no. 4, pp. 282–290, 2012.

[29] *Fingerprints,* http://www.forensic-medecine.info/fingerprints.html.

[30] *[FVC2004] The 3rd Fingerprint Verification Competition,* http://bias.csr.unibo.it/fvc2004/, accessed: November 6, 2012.

[31] *NIST Special Database 27,* http://www.nist.gov/srd/nistsd27.cfm.

[32] M.A. Wahby Shalaby and M. O. Ahmad, "A multilevel structural technique for fingerprint representation and matching," *Signal Processing,* vol. 93, no. 1, pp. 56–69, 2013.

[33] N.K. Ratha, C. Shaoyun, and A.K. Jain, "Adaptive flow orientation-based feature extraction in fingerprint images," *Pattern Recognition,* vol. 28, no. 11, pp. 1657–1672, 1995.

[34] Vijay Kumar Emani, "Curvelet transform-based techniques for biometric person identification", A master's thesis from Concordia University, Canada.

[35] *[FVC2000] The 2nd Fingerprint Verification Competition,* http://bias.csr.unibo.it/fvc2000/, accessed: November 6, 2012.

[36] *[FVC2002] The 4th Fingerprint Verification Competition,* http://bias.csr.unibo.it/fvc2002/, accessed: November 6, 2012.

[37] Gottschlich, C., Mihaˇilescu, P., Munk, A.: "Robust orientation field estimation and extrapolation using semilocal line sensors", IEEE Transaction on Information Forensics and Security, vol. 4, no. 4, pp. 802–811, 2009.

[38] Kass, M., Witkin, A.: "Analyzing oriented patterns", Computer Vision, Graphics and Image Processing, vol. 37, no. 3, pp. 362–385, 1987.

[39] Bazen, A.M., Gerez, S.H.: "Systematic methods for the computation of the directional fields and singular points of fingerprints", IEEE Trans. Pattern Analysis and Machine Intelligence., vol. 24, no. 7, pp. 905–919, 2002.

[40] R.C. Gonzalez and R.E. Woods, "Digital Image Processing," 3rd ed., Prentice-Hall, 1989.

[41] H. Fronthaler, K. Kollreider, J. Bigun, J. Fierrez, F. A. Fernandez, J.O. Garcia and J. G. Rodriguez, "Fingerprint image quality estimation and its application to multialgorithm verification," IEEE Transaction on Information Forensics and Security, vol. 3, no. 2, pp. 331-338, 2008.

[42] J. Abraham, P. Kwan, J. Gao, "Fingerprint Matching using a Hybrid Shape and Orientation Descriptor," State of the art in Biometrics, pp. 25–56, 2011.

[43] Z. Shi and V. Govindaraju, "A chaincode based scheme for fingerprint feature extraction," *Pattern Recognition,* vol. 40, no. 1, pp. 198-211, 2007.

[44] F. L. Bookstein, "Principal warps: Thin-plate splines and the decomposition of deformations," *IEEE Trans. Pattern Analysis and Machine Intelligence.,* vol. 11, no. 6, pp. 568-585, 1989.

Appendix I

Values of the parameters used in the simulation of the proposed enhancement scheme

First Stage	
Gradient operator	Gaussian
Mask size	7×7
Multiplying factor, M_P	0.25
Strength of diffusion, a	0.01
Step size, T	0.25
Number of iterations	10
Second Stage	
Desired mean, M_0	128
Desired variance, V_0	16384
α	100
β	1
w	3
h	9
Third Stage	
Spectral window	Gaussian
BLKSZ	12
OVRLP	6
WNDSZ=BLKSZ+2*OVRLP	24
Size of FFT	32
C_φ	$(3/\pi)^2\ln(2)$